iScience

CellPress
OPEN ACCESS

Article

Signal Decoding for Glutamate Modulating Egg Laying Oppositely in *Caenorhabditis elegans* under Varied Environmental Conditions

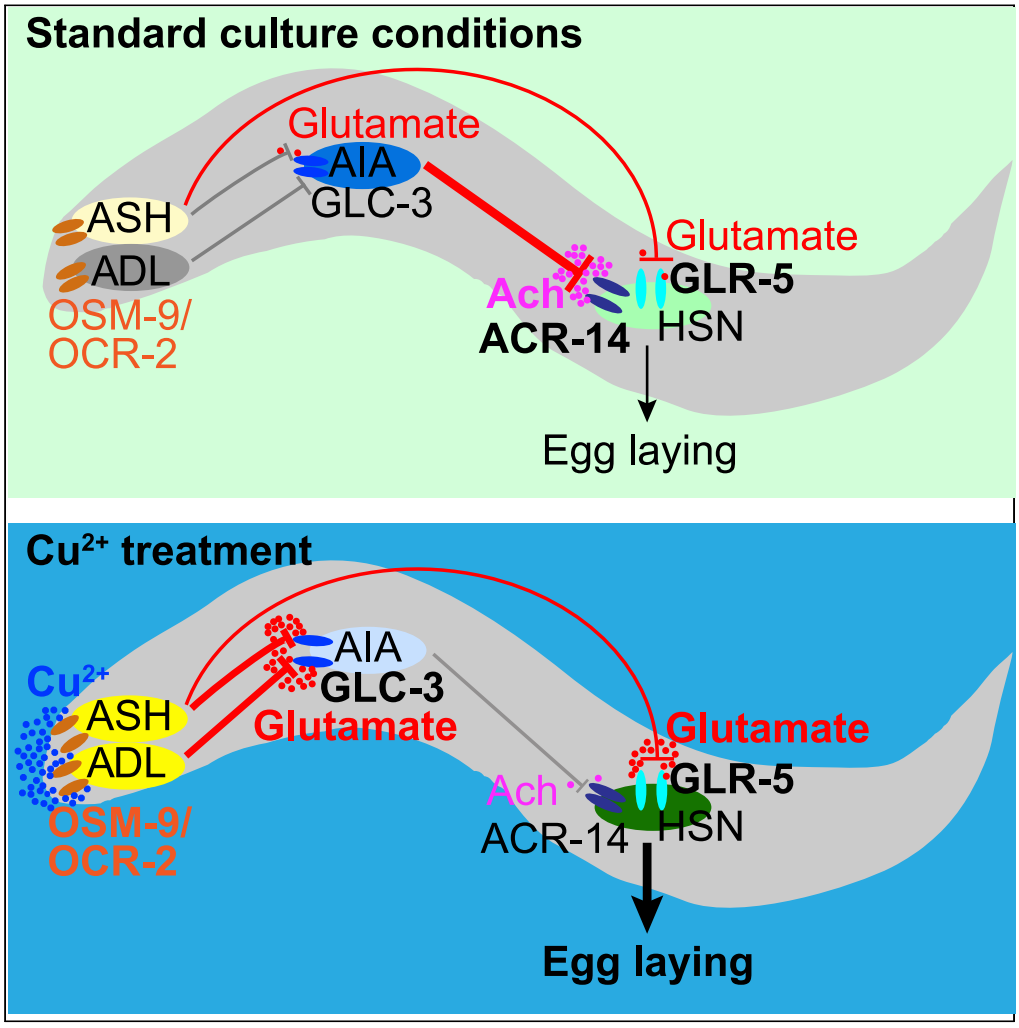

Xin Wen, Yuan-Hua Chen, Rong Li, ..., Ping-Zhou Wang, Einav Gross, Zheng-Xing Wu

einavg@ekmd.huji.ac.il (E.G.)
ibbwuzx@mail.hust.edu.cn (Z.-X.W.)

HIGHLIGHTS

Short-term exposure of $CuSO_4$ evokes hyperactive egg laying

ASHs inhibit HSNs and egg laying via GLR-5 receptor under no Cu^{2+} treatment

AIA interneurons suppress HSNs and thus egg laying through ACR-14 signaling

Under noxious Cu^{2+} treatment, ASHs and ADLs suppress AIAs and augment egg laying

Wen et al., iScience *23*, 101588
October 23, 2020
https://doi.org/10.1016/j.isci.2020.101588

iScience

CellPress
OPEN ACCESS

Article

Signal Decoding for Glutamate Modulating Egg Laying Oppositely in *Caenorhabditis elegans* under Varied Environmental Conditions

Xin Wen,[1,3] Yuan-Hua Chen,[1,3] Rong Li,[1,3] Ming-Hai Ge,[1] Sheng-Wu Yin,[1] Jing-Jing Wu,[1] Jia-Hao Huang,[1] Hui Liu,[1] Ping-Zhou Wang,[1] Einav Gross,[2,*] and Zheng-Xing Wu[1,4,*]

SUMMARY

Animals' ability to sense environmental cues and to integrate this information to control fecundity is vital for continuing the species lineage. In this study, we observed that the sensory neurons Amphid neuron (ASHs and ADLs) differentially regulate egg-laying behavior in *Caenorhabditis elegans* under varied environmental conditions via distinct neuronal circuits. Under standard culture conditions, ASHs tonically release a small amount of glutamate and inhibit Hermaphrodite specific motor neuron (HSN) activities and egg laying via a highly sensitive Glutamate receptor (GLR)-5 receptor. In contrast, under Cu^{2+} stimulation, ASHs and ADLs may release a large amount of glutamate and inhibit Amphid interneuron (AIA) interneurons via low-sensitivity Glutamate-gated chloride channel (GLC)-3 receptor, thus removing the inhibitory roles of AIAs on HSN activity and egg laying. However, directly measuring the amount of glutamate released by sensory neurons under different conditions and assaying the binding kinetics of receptors with the neurotransmitter are still required to support this study directly.

INTRODUCTION

The establishment of a succeeding generation is essential for the survival of all biological species. Therefore, it is of paramount importance for animals to breed, undergo pregnancy, and give birth to offspring at the right time and place. In this context, environmental conditions are of great importance since unsuitable environmental conditions cannot support the development of offspring. For this reason, animals must sense their environment, integrate sensory information, and translate the information into the reproductive process.

Remarkably, some animal species increase their reproduction rates in response to environmental stresses. For example, *Acheta domesticus* crickets increase egg laying in response to infections with bacteria and parasites (Adamo, 1999). Also, *Drosophila nigrospiracula* males infected experimentally by parasites courted females significantly more than unparasitized control males before dying, albeit they lived a shorter life than the control males. This higher courtship results in an increased mating rate and potentially greater reproductive success (Polak and Starmer, 1998). *Culex pipiens* mosquitoes infected with the parasite *Plasmodium relictum* bring forward their oviposition schedule (Vezilier et al., 2015). Freshwater *Pomacea canaliculata* snails produce eggs earlier in the presence of *Trachemys scripta elegans* predators (Guo et al., 2017). Intensive harvesting has caused pronounced shifts in growth rate, reproductive timing, and even genomic shifts in many commercially valuable stocks (Allendorf and Hard, 2009; Baskett and Barnett, 2015; Eikeset et al., 2016; Heino et al., 2015; Therkildsen et al., 2019). These observations and many others could be explained by the life-history theory, which argues that when organisms experience environmental conditions that can reduce their long-term reproductive success, they increase their present reproductive output through phenotypic plasticity (Dingle, 1990; Fox et al., 2019; Hirshfield and Tinkle, 1975; Kavanagh and Kahl, 2016; Neil and Ford, 1989). However, the molecular and neuronal mechanisms underlying this adaptive response have not been fully elucidated.

Both genes and the modalities of neuroinformation integration are conserved among animal genera. Experimentally tractable animal models are generally used to study the relationships among the genes, proteins, and neural circuits underlying behaviors. The nematode *Caenorhabditis elegans* (*C. elegans*) is a favored

[1]Key Laboratory of Molecular Biophysics of Ministry of Education, Institute of Biophysics and Biochemistry, College of Life Science and Technology, Huazhong University of Science and Technology, Wuhan, China

[2]Department of Biochemistry & Molecular Biology, IMRIC, Faculty of Medicine, The Hebrew University of Jerusalem, Jerusalem, Israel

[3]These authors contributed equally

[4]Lead Contact

*Correspondence: einavg@ekmd.huji.ac.il (E.G.), ibbwuzx@mail.hust.edu.cn (Z.-X.W.)

https://doi.org/10.1016/j.isci.2020.101588

model for behavioral studies because of its compact nervous system and experimental tractability (de Bono and Maricq, 2005). The *C. elegans* hermaphrodite nervous system consists of merely 302 neurons and 7,446 synapses (Cook et al., 2019; https://www.wormatlas.org; White et al., 1986). Egg laying in *C. elegans* is a process by which hermaphrodites deposit developing embryos into the environment. A small network of motor neurons (two HSNs and six ventral nerve cord [VC] motor neurons) and specialized smooth muscle cells (four vulval vm2, four vulval vm1, and eight uterine muscle cells) control the laying of eggs. HSNs play a central role in egg-laying behavior. These neurons not only control vm2 vulval muscles and direct synaptic output to VC5 motor neurons but also receive synaptic input from the rest of the nervous system and feedback from muscle cells (Collins et al., 2016; Collins and Koelle, 2013; Schafer, 2005, 2006; Zhang et al., 2008, 2010). The tight regulation of egg laying results in adaptive egg laying and coordination with other behaviors (de Bono and Maricq, 2005; Schafer, 2005). Egg laying is regulated by HSNs through a number of neurotransmitters: serotonin (Greenwald and Horvitz, 1982), acetylcholine (Duerr et al., 2001), and at least three neuropeptides encoded by *flp-19*, *nlp-3*, and *nlp-15* (Brewer et al., 2019; Kim and Li, 2004; Nathoo et al., 2001; Schafer, 2006). Serotonin stimulates vulval muscle activity by increasing the frequency of spontaneous calcium transients (Shyn et al., 2003). Two serotonin receptors, SER-1 and SER-7, appear to be involved in activating vulval muscle activity (Dempsey et al., 2005; Hobson et al., 2006). HSNs also receive humoral modulation from endocrine uv1 cells, which release tyramine (Alkema et al., 2005), and the neuropeptides FMRFamide-related neuropeptides (FLP-11 and FLP-22) (Kim and Li, 2004).

Many environmental factors affect the rate and temporal pattern of egg laying. Food supply affects egg-laying behavior. *C. elegans* lays more eggs in the presence of abundant food than in the absence of food (Trent et al., 1983). Gentle touch inhibits egg laying (Sawin, 1996; Zhang et al., 2008) via sensation in the touch receptor nterior lateral microtubule cell (ALM) and Posterior lateral microtubule cell (PLM) neurons (Zhang et al., 2008). High and low osmolarity enhances and suppresses egg-laying and spike frequency in the HSN and VC motor neurons, respectively (Zhang et al., 2008). High glucose reduces the egg-laying rate (Teshiba et al., 2016). High environmental CO_2 (5%) inhibits egg laying and activity in HSNs by activating CO_2-sensitive Amphid wing cell (AWC) neurons (and possibly other sensory neurons) via guanylate cyclase-9 (GCY-9)-TAX-2/TAX-4 signaling (Fenk and de Bono, 2015). Predator-secreted sulfolipids suppress egg laying for many minutes after exposure, as mediated by TAX-4 signaling in sensory Amphid neurons (ASI and ASJ) (Liu et al., 2018). *C. elegans* responds to environmental stresses to augment its egg laying, similar to other animals. Approximately 48 hr of exposure to teratogens (such as nicotine, cadmium, and tributyltin) at low doses increases the egg-laying rate (Killeen and Marin de Evsikova, 2016). However, possibly due to toxicity, long-term exposure to high levels (100 and 500 μM) of $CuSO_4$ decreased worm brood size and led to internal hatching of offspring inside their mothers (bagging) (Calafato et al., 2008). Conversely, short-term (<6 hr) exposure to cadmium ions increased the worm's egg-laying rate (Killeen and Marin de Evsikova, 2016). However, the neural mechanisms, i.e., map and neurosignal integration in neural circuits governing the regulation of egg laying by environmental cues, have not been fully elucidated.

The polymodal ASH sensory neurons are primary nociceptor neurons. These neurons are involved in sensing a variety of aversive stimuli and mediating the avoidance of high osmotic, mechanical, and chemical stimuli (Bargmann et al., 1990; Bargmann, 2006; Guo et al., 2015; Hart et al., 1995; Hilliard et al., 2005; Kaplan and Horvitz, 1993). The sensory neurons ADLs, Amphid neuron (ASKs, and ASEs) play minor roles in the sensation of aversive cues and avoidance behavior from heavy-metal ions Cd^{2+} and Cu^{2+}, odors (octanol), high osmotic strength, and Sodium dodecyl sulfate (SDS) (Bargmann et al., 1990; de Bono and Maricq, 2005; Hilliard et al., 2002; Sambongi et al., 1999; Troemel et al., 1995). ASHs and ADLs play primary and secondary roles in sensing and avoiding heavy metals (Sambongi et al., 1999). These neurons sense Cu^{2+} via OSM-9 and capsaicin receptor-related (OCR-2)/osmotic avoidance abnormal (OSM-9) signaling. The transient receptor potential cation channel, subfamily V (TRPV) proteins OCR-2 and OSM-9, which may assemble into a single channel complex (Tobin et al., 2002), mediate the nociception of Cu^{2+} (Guo et al., 2018; Hilliard et al., 2005; Kahn-Kirby and Bargmann, 2006; Sambongi et al., 1999; Wang et al., 2015). ASHs and ADLs modulate Cu^{2+} avoidance primarily via glutamatergic signaling (Choi et al., 2015; Mellem et al., 2002). Glutamate is an essential neurotransmitter in the vertebrate and invertebrate nervous systems. Glutamate signaling modulates a broad range of behaviors mediated by diverse receptors in *C. elegans* (Whittaker and Sternberg, 2004). Glutamate is involved in the regulation of a broad spectrum of behaviors. Examples include salt chemotaxis (Chalasani et al., 2007), habituation in tap-withdrawal response (Rankin and Wicks, 2000), local search (Hills et al., 2004), cryophilic response (Clark et al., 2007), and pumping inhibition by and initiation of avoidance of quinine (Zou et al., 2018). The functions of glutamate in the regulation of egg laying have not been determined.

In this study, we utilized *C. elegans* to explore the effects of metal ions on egg laying in *C. elegans*. We found that short-term (30 min) treatments with the metal ions tested, that is, Cu^{2+}, Ni^{2+}, Mn^{2+}, and Fe^{3+}, induced hyperactive egg laying. Using genetic analyses, behavioral tests, genetic and chemogenetic manipulation of neurons, neuronal calcium imaging, and pharmacological tests, we dissected the molecular and neurocircuit mechanisms underlying the effect of Cu^{2+}. We also analyzed the mechanisms by which sensory information is encoded, decoded, and translated into behavior.

RESULTS

Noxious Stimulation of $CuSO_4$ Evokes Hyperactive Egg Laying and HSN Calcium Signals via the OCR-2/OSM-9 Channel Complex in ASH and ADL Sensory Neurons in *C. elegans*

Heavy-metal ions, such as Cu^{2+}, Ni^{2+}, Mn^{2+}, and Fe^{3+}, are common environmental contaminants. These ions are harmful to animals at high contents. We examined the *C. elegans* egg-laying rate under short-term exposure to Cu^{2+} ($CuSO_4$), Ni^{2+} ($NiCl_2$), Mn^{2+} ($MnCl_2$), and Fe^{3+} ($Fe_2(SO_4)_3$) ions at 100 μM. A 30-min exposure of Cu^{2+}, Ni^{2+}, Mn^{2+}, and Fe^{3+} at 100 μM significantly increased the number of eggs laid in *C. elegans* (Figure S1A). We used 30 min of administration of these metal ions based on our time course assay of Cu^{2+}. The number of eggs laid significantly increased upon exposure to 100 μM $CuSO_4$ for 10 min, 20 min, and 30 min and then decreased thereafter (Figure 1A). $CuSO_4$ (Cu^{2+}) is a commonly used noxious chemical in studies of nociception and avoidance in *C. elegans*. Thus, we used 30 min of treatment with Cu^{2+} as stimulation (subsequent short-term Cu^{2+} treatment) in our following tests. The egg-laying rate responded dose-dependently to the short-term challenges of Cu^{2+} at various concentrations, which was accurately fitted by a Hill function with concentration for 50% of maximal effect (EC_{50}) = 4.68 μM, Figure 1B). Adult hermaphrodites generally have a store of 10–15 eggs in their uterus at any given time (Schafer, 2005). Augmented egg laying increases the eggs laid at early developmental stages (Alkema et al., 2005; Ringstad and Horvitz, 2008). Short-term Cu^{2+} treatment notably increased the number of eggs at the 1–8 and 9–20 cell stages (Figures 1C and 1D). We summed the ratios of the eggs at these two embryonic stages and indicated them as early eggs. Egg laying is controlled by HSN command motor neurons (de Bono and Maricq, 2005; Schafer, 2005; Collins et al., 2016; Desai and Horvitz, 1989; Trent, 1983; Zhang et al., 2008, 2010). Cu^{2+} treatment should excite HSNs. Thus, we employed calcium imaging to examine HSN activity in response to the acute application of Cu^{2+} at various concentrations using immobilized worms glued onto a Polydimethylsiloxane (PDMS) pad attached to a cover glass, as previously described (Zhang et al., 2008). As shown in Figures 1E and 1F, Ca^{2+} signals in HSNs dose-dependently increased in response to $CuSO_4$ stimuli (well fitted by the Hill function with EC_{50} = 2.46 μM). Interestingly, the HSN Ca^{2+} signals and the egg-laying rates correlated linearly (Pearson r = 0.9845, Figure 1G).

Nociceptor ASHs and ADLs sense Cu^{2+} and mediate avoidance of this ion via the OCR-2/OSM-9 complex. These neurons and molecules are likely involved in the augmentation of egg laying by Cu^{2+}. Next, we used *ocr-2* and *osm-9* mutants and genetically rescued worms to test the functional roles of this channel complex in the modulation of egg laying and HSN activity. No ASH-specific promoter was identified. Therefore, we used an FLP-out (a recombinase-catalyzed intramolecular excision of spacer DNA between tandemly oriented transcriptional terminator flanked by FLP recognition [FRT] sites) system to drive specific expression of TeTx in ASH neurons. The system is based on the FLP-out of a transcriptional terminator (Davis et al., 2008; Guo et al., 2015; Macosko et al., 2009; Voutev and Hubbard, 2008). When worms expressed both *sra-6p*::*flp*::*unc-54* 3′UTR and *gpa-11p*::*FRT*::*stop*::*FRT*::*ocr-2*(or *osm-9*)::*sl2*::*GFP* constructs, FLP recombinase driven by the *sra-6* promoter excised the FRT-flanked transcriptional terminator and drove *ocr-2* or *osm-9* directed by *gpa-11p* to express specifically in ASHs (Figure S1B). Our results showed that the *ocr-2*(*ak47*) and *osm-9*(*tm5418*) mutants and all transgenic worms with neuron-specific genetic rescue (reconstitution) of *ocr-2* or *osm-9* had no defects in egg laying or HSN Ca^{2+} signals under normal culture conditions. However, the mutants lost the responses of egg-laying behavior and HSN Ca^{2+} transients to the short-term and acute treatments of Cu^{2+} at 100 μM (subsequent acute Cu^{2+} treatment), respectively. The reconstitution of both genes in ASHs or ADLs alone or in both neurons, although not in other neurons, restored wild-type phenotypes in both activities (Figures 2A–2F and S1C–S1F). In addition, ADLs displayed a mild increase in Ca^{2+} transients in response to stimulation with 100 μM Cu^{2+} (Figure S1C). These results indicate that primary ASH and secondary ADL sensory neurons sense Cu^{2+} via OCR-2/OSM-9 signaling and upregulate egg laying in *C. elegans*.

ASH and ADL Sensory Neurons Regulate Egg Laying and HSN Activity Differently under Standard Culture Conditions and Cu^{2+} Treatment

ASHs and ADLs play roles in avoidance of heavy metals, primarily via glutamatergic signaling (Choi et al., 2015; Mellem et al., 2002; Sambongi et al., 1999). ASHs and HSNs but not ADLs and HSNs connect with

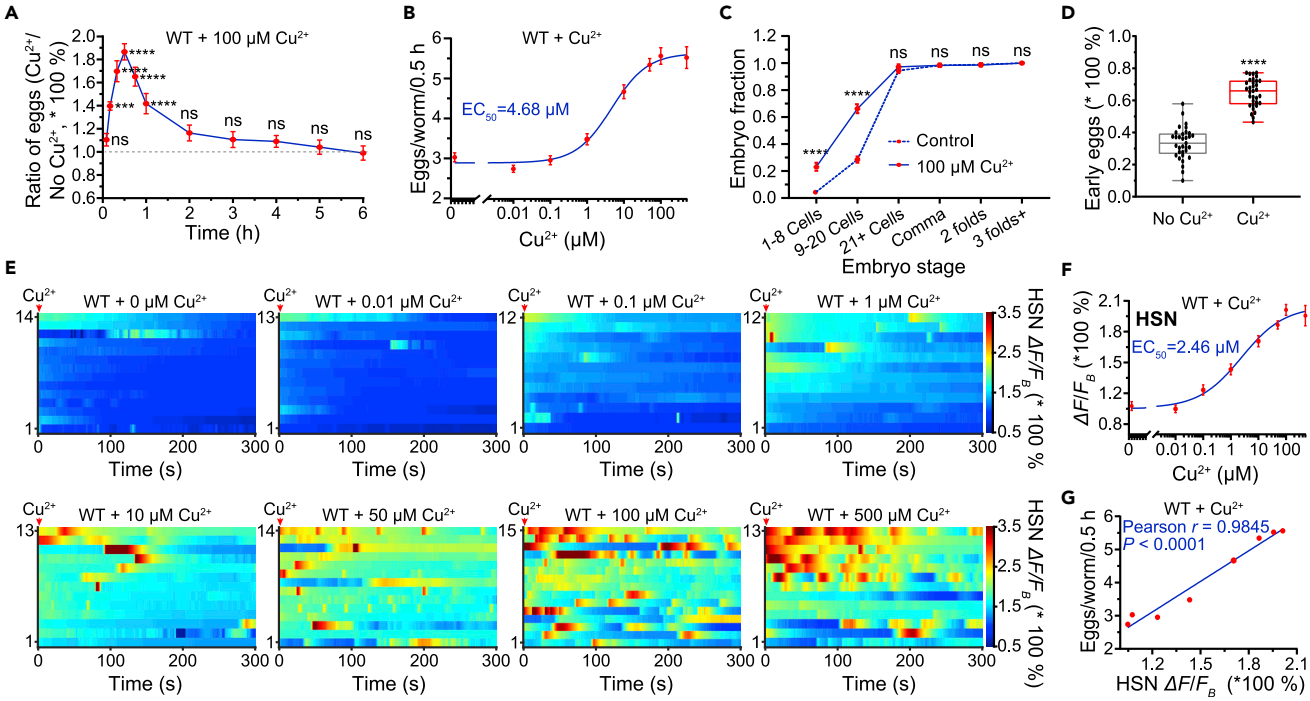

Figure 1. Cu^{2+} Evokes Hyperactive Egg Laying and Augments Calcium Signals in HSN Motor Neurons in *C. elegans*

(A) The ratio of the eggs laid (the egg number in Cu^{2+}-treated worms/that in Cu^{2+}-untreated animals) under treatment of 100 μM Cu^{2+} for various durations (5 min, 10 min, 20 min, 30 min, 45 min, 1 hr, 2 hr, 3 hr, 4 hr, 5 hr, and 6 hr) in wild-type N2 worms. Data are expressed as means ± SEM. Statistical significance of difference was analyzed by one-way ANOVA with the post hoc test of Dunnett's multiple comparison correction in comparison of a hypothesized ratio (= 1) in Cu^{2+}-untreated worms and indicated as follows: ns = not significant, ***$p < 0.001$ and ****$p < 0.0001$.

(B) The number of the eggs laid per worm per 30 min (egg-laying rate) under application of $CuSO_4$ (Cu^{2+}) at various concentrations (in μM: 0, 0.01, 0.1, 1, 10, 50, 100, and 500) in WT worms. The solid blue line indicated the Hill-function fitting. Data are expressed as means ± SEM.

(C) Cumulative percent of the eggs at different embryo stages (1–8 cells, 9–20 cells, 21 + cells, comma, two folds, and three folds+) in WT worms treated without versus with 100 μM Cu^{2+}. Data are expressed as means ± SEM. Statistical significance of difference was analyzed by two-way ANOVA with post hoc Sidak's multiple comparisons test in the comparison between the data from Cu^{2+}-untreated and Cu^{2+}-treated worms, and indicated as follows: ns = not significant and ****$p < 0.0001$.

(D) Percent of the eggs at early developmental stages (stages of 1–8 cells and 9–20 cells) in WT worms treated without and with 100 μM $CuSO_4$. Data are displayed in box plots, with each dot representing the data from each individual tested animal. Statistical significance of difference was analyzed by unpaired *t* test.

(E) Heat maps of percent changes in somal calcium (Ca^{2+}) transients in HSN motor neurons in WT worms treated with $CuSO_4$ (Cu^{2+}) at various concentrations for 5 min $\Delta F = F - F_B$. *F*, the average fluorescence intensity of the region of interest (ROI) of an HSN soma in each frame; F_B, a background signal defined as the average fluorescence intensity of ROI adjacent to the HSN soma in all frames. The label on the left y axis indicates the number of tested worms.

(F) Hill plot of the somal HSN Ca^{2+} signals in WT worms treated with $CuSO_4$ at various concentrations shown in (E). Data are expressed as means ± SEM.

(G) Linear correlation between the egg-laying rates and the HSN somal Ca^{2+} signals in WT worms treated with Cu^{2+} at varied concentrations (in μM: 0, 0.01, 0.1, 1, 10, 50, 100, and 500).

See also Figure S1 and Table S1.

each other via chemosynapses (Cook et al., 2019; https://www.wormatlas.org; White et al., 1986). The vesicular glutamate transporter EAT-4 is essential for glutamate filling in synaptic vesicles (Bellocchio et al., 2000; Lee et al., 1999). Thus, we employed an *eat-4* mutant to test glutamate regulation of egg laying and HSN activity. Interestingly, the *eat-4*(*ky5*) mutant exhibited the maximum egg-laying rate and HSN Ca^{2+} signals under both standard culture conditions and Cu^{2+} treatments. Genetic rescuing of *eat-4* in ASHs alone but not in ADLs restored the wild-type phenotypes, including egg-laying and HSN activity in the transgenes under both conditions. The *eat-4* rescue in ADLs even augmented both Cu^{2+}-elicited activities (Figures 3A–3C and S3A). However, this observation may be attributable to EAT-4 overexpression. The reconstitution of *eat-4* in other *eat-4*-expressing sensory neurons, such as ADFs, ASKs, ASJs, and AWCs, had no impact under either state (S2A and S2B). Taken together, this set of results suggests that ASHs and ADLs modulate egg-laying behavior differently. Next, we set out to identify the glutamatergic receptor(s) involved in egg-laying regulation. Among the mutants that we tested, *glr-5*(*tm3506*) displayed

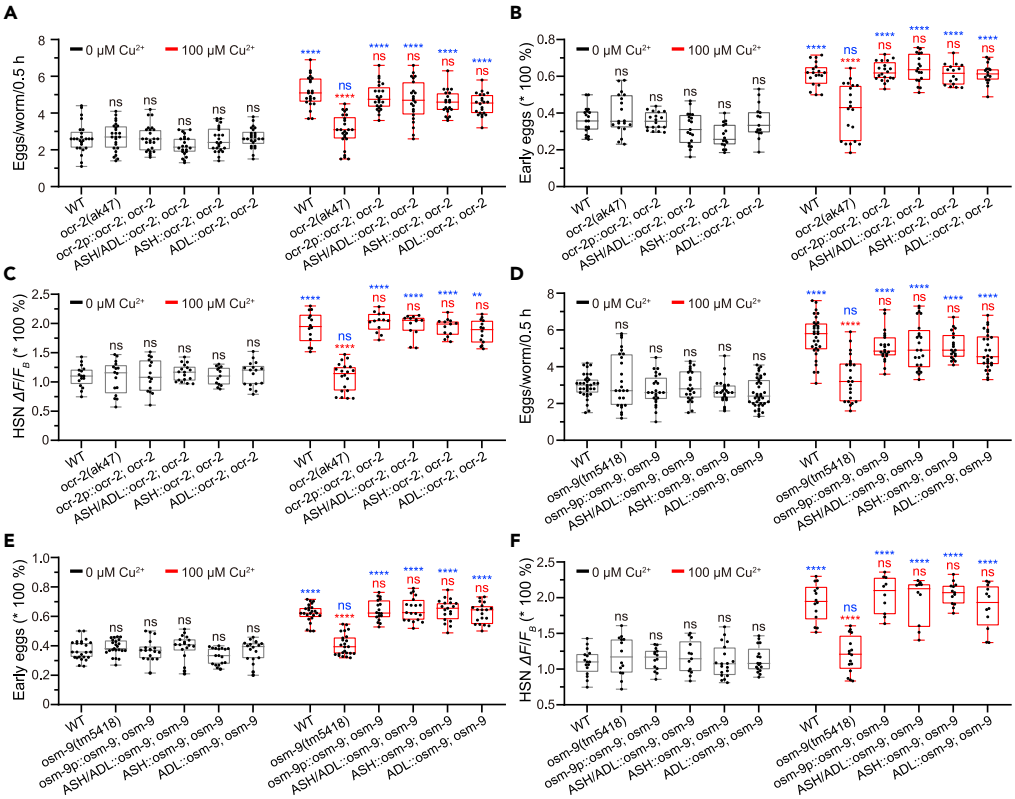

Figure 2. Sensory ASH and ADL Neurons Response to Cu^{2+} Treatment and Regulate Egg Laying Activity in HSN Motor Neurons through OSM-9/OCR-2 Signaling

(A–F) The number of the eggs laid per worm per 30 min (egg-laying rate, A and D), percent of the eggs at early developmental stages (both 1–8 cells and 9–20 cells, B and E), and the somal HSN calcium signals (C and F) in the worms of indicated genotypes treated without (in black) or with (in red) 100 μM $CuSO_4$. $\Delta F = F - F_B$. F, the average fluorescence intensity of the region of interest (ROI) of an HSN soma in each frame; F_B, a background signal defined as the average fluorescence intensity of ROI adjacent to the HSN soma in all frames.

All Data are displayed as box plots with each dot representing the data from each individual tested worm. Statistical significance of difference was analyzed by two-way ANOVA analysis with the post hoc test of Tukey's multiple comparison correction and indicated as follows: ns = not significant, ****$p < 0.0001$, and in different colors for varied comparisons. Black or red, a comparison of tested worms with the control (wild type N2) under Cu^{2+}-untreated or Cu^{2+}-treated conditions; blue, that of Cu^{2+}-untreated with Cu^{2+}-treated animals of the same genotype.

See also Figure S1 and Table S1.

defects in egg laying under standard culture conditions and short-term Cu^{2+} treatment, while *glc-3*(*ok321*) showed behavioral abnormalities only under Cu^{2+} treatment (Figures S2C and S2D). We first focused on the *glr-5* gene, which encodes a GLR-5 glutamate receptor. GLR-5 is a kainate (non-NMDA)-type ionotropic receptor subunit (Brockie et al., 2001; Brockie and Maricq, 2003). GLR-5 is expressed in interneurons and motoneurons, including HSNs and VCs (https://wormbase.org). We employed mutants of *glr-5*(*tm3506*) single mutant, *eat-4*(*ky5*); *glr-5*(*tm3506*) double mutant, and *eat-4* and *glr-5* rescued worms to further test the regulatory roles of glutamatergic signaling in modulating egg laying and HSN activity. Expressing *glr-5* in all *glr-5*-expressing cells (under its promoter region) or HSNs directed by the *egl-6a* promoter (Emtage et al., 2012) restored the wild-type phenotypes (Figures 3D–3F and S3A). The *eat-4*; *glr-5* double mutant displayed similar phenotypes to *eat-4*(*ky5*). However, this mutant showed different phenotypes than *glr-5*(*tm3506*). Only dual reconstitution of both *eat-4* in ASHs and *glr-5* in HSNs (in worms of ZXW1425 strain, its genotype showed in Table S1), neither single re-expression of *eat-4* in ASHs nor *glr-5* in HSNs, restored wild-type phenotypes (Figures 3G–3I and S3B).

To specifically block neurotransmission in ASHs, we used the tetanus toxin system (TeTx). TeTx is a specific protease of synaptobrevin (Schiavo et al., 1992) that blocks vesicle fusion with the plasma membrane and

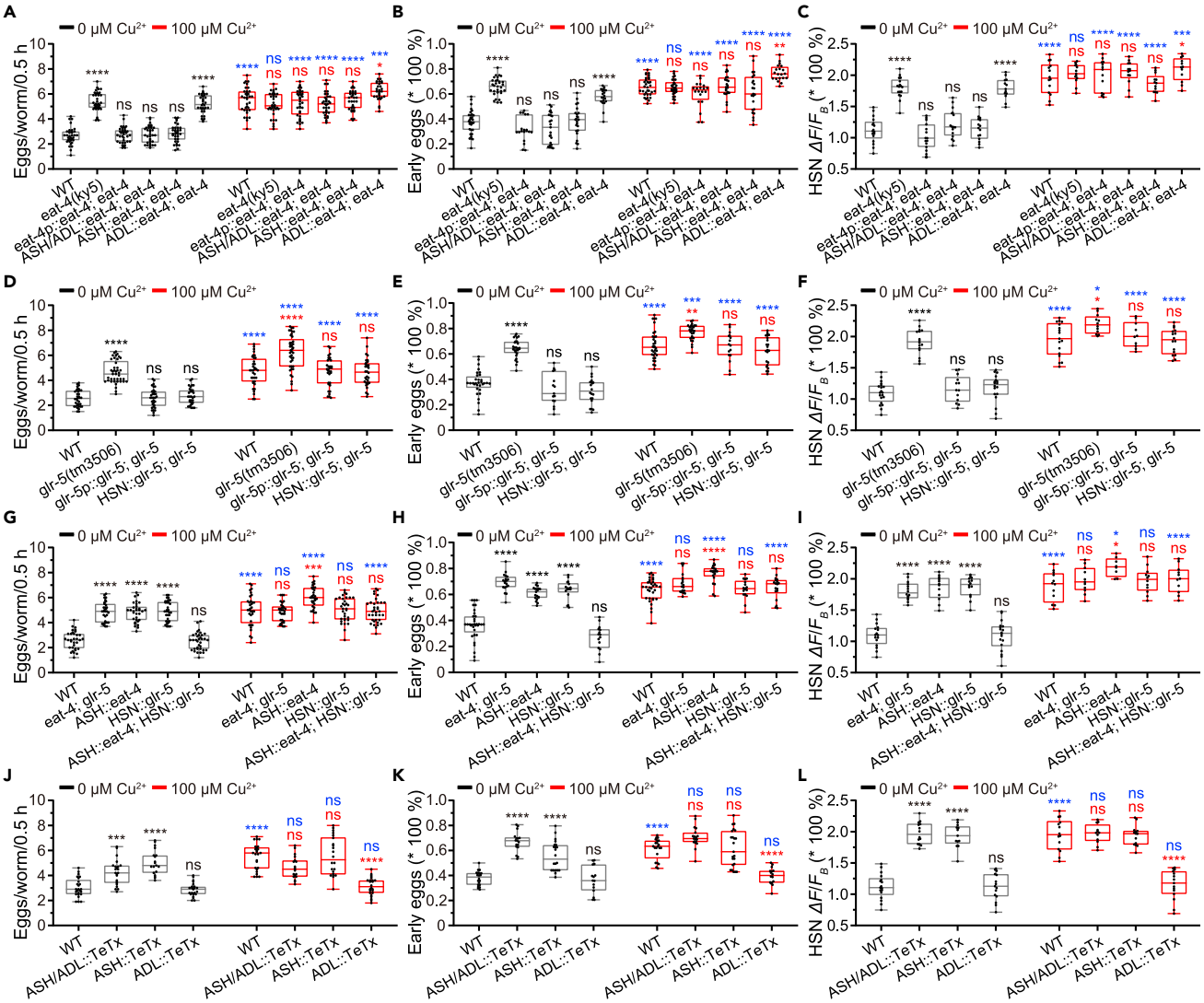

Figure 3. Sensory ASH Neurons Differently Modulate Egg-Laying and HSN Activity under Standard Culture Conditions and Cu^{2+} Treatment via Glutamatergic GLR-5

(A–L) The number of the eggs laid per worm per 30 min (egg-laying rate, A, D, G, and J), percent of the eggs at early developmental stages (both 1–8 cells and 9–20 cells, B, E, H, and K), and the HSN somal calcium signals (C, F, I, and L) in the worms of indicated genotypes treated without (in black) or with (in red) 100 μM $CuSO_4$. $\Delta F = F - F_B$. F, the average fluorescence intensity of the region of interest (ROI) of an HSN soma in each frame; F_B, a background signal defined as the average fluorescence intensity of ROI adjacent to the HSN soma in all frames.

All Data are displayed as box plots with each dot representing the data from each individual tested worm. Statistical significance of difference was analyzed by two-way ANOVA analysis with the post hoc test of Tukey's multiple comparison correction and indicated as follows: ns = not significant, $*p < 0.05$, $**p < 0.01$, $***p < 0.001$, $****p < 0.0001$, and in different colors for varied comparisons. Black or red, a comparison of tested worms with the control (wild type N2) under Cu^{2+}-untreated or Cu^{2+}-treated conditions; blue, that of Cu^{2+}-untreated with Cu^{2+}-treated worms of the same genotype.

See also Figures S2–S4 and Table S1.

thus neurotransmission. The TeTx system has been used successfully in neurobiological studies to inhibit chemical synaptic transmission in tested neurons (subsequent neuron::*TeTx* in short) in *C. elegans* (Guo et al., 2015, 2018; Liu et al., 2019; Macosko et al., 2009; Wang et al., 2016). As expected, ASH::*TeTx* resulted in defects in egg-laying and HSN Ca^{2+} signals in both Cu^{2+}-untreated and Cu^{2+}-treated worms. However, ADL::*TeTx* resulted in normal egg laying and HSN activity under standard culture conditions and loss of the responses of both activities to Cu^{2+} treatments (Figure 3J–3L and S3C). However, the expression of TeTx in other sensory neurons, except ASIs, did not significantly affect egg-laying behavior (Figures S4A and S4B).

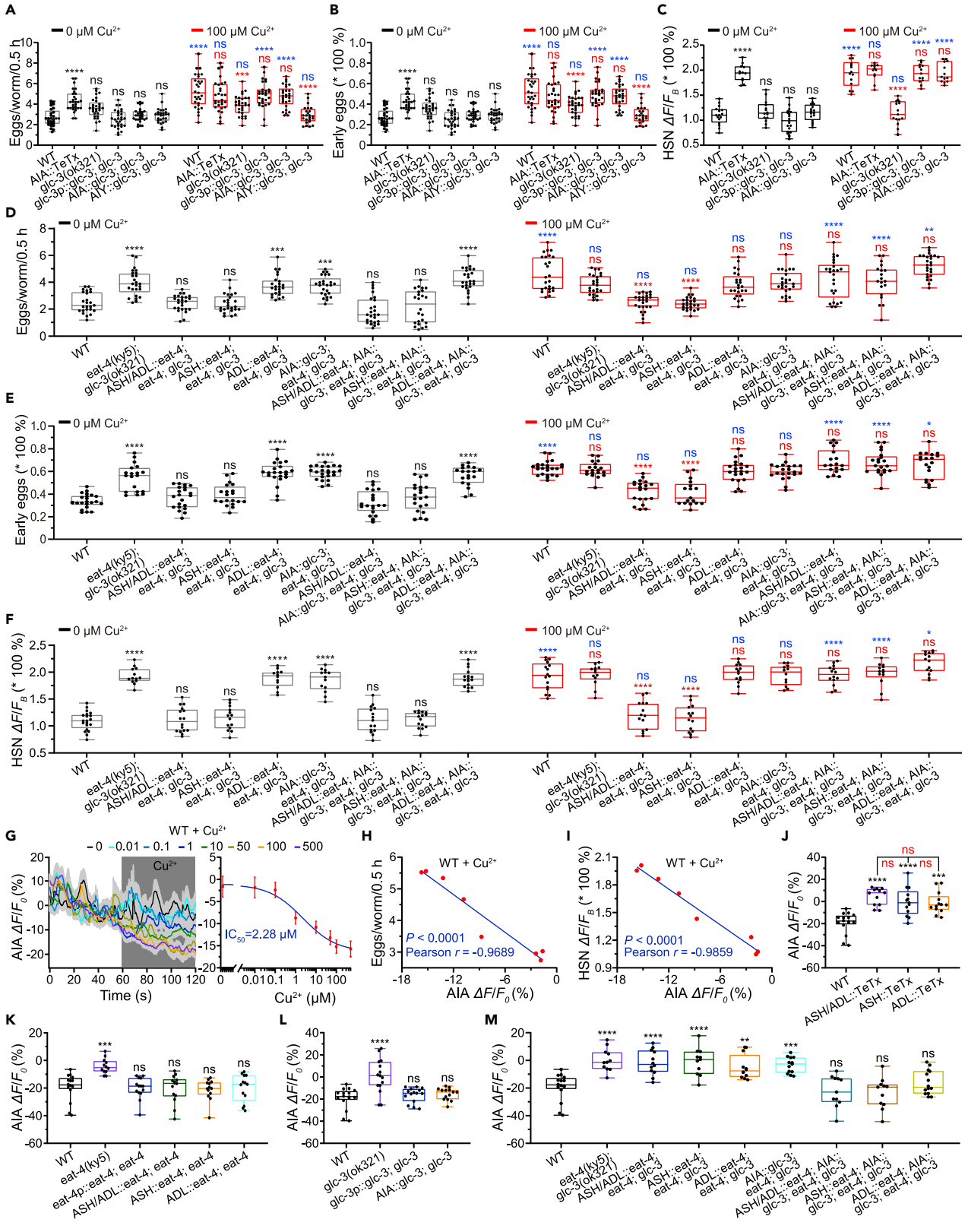
A
0 μM Cu2+
100 μM Cu2+
Eggs/worm/0.5 h
WT
AIA::TeTx
glc-3(ok321)
glc-3p::glc-3; glc-3
AIA::glc-3; glc-3
AIY::glc-3; glc-3
B
Early eggs (* 100 %)
C
HSN ΔF/F0 (* 100 %)
D
E
F
G
WT + Cu2+
0 0.01 0.1 1 10 50 100 500
AIA ΔF/F0 (%)
Time (s)
IC50=2.28 μM
Cu2+ (μM)
H
Eggs/worm/0.5 h
P < 0.0001
Pearson r = -0.9689
AIA ΔF/F0 (%)
I
HSN ΔF/F0 (* 100 %)
P < 0.0001
Pearson r = -0.9859
J
AIA ΔF/F0 (%)
WT
ASH/ADL::TeTx
ASH::TeTx
ADL::TeTx
K
WT
eat-4(ky5)
eat-4p::eat-4; eat-4
ASH/ADL::eat-4; eat-4
ASH::eat-4; eat-4
ADL::eat-4; eat-4
L
WT
glc-3(ok321)
glc-3p::glc-3; glc-3
AIA::glc-3; glc-3
M
WT
eat-4(ky5)
glc-3(ok321)
ASH/ADL::eat-4; eat-4
ASH::eat-4; eat-4
ADL::eat-4; eat-4
AIA::glc-3; eat-4
ASH/ADL::eat-4; AIA::glc-3; eat-4
ASH::eat-4; AIA::glc-3; eat-4
ADL::eat-4; AIA::glc-3; eat-4

Figure 4. AIA Interneurons Mediate Cu^{2+}-evoked Augment of Egg-Laying and HSN Activity via GLC-3 Signaling

(A–F) Egg-laying rates (A and D), percent of eggs at early development stages (B and E), and percent changes in the HSN calcium signals (C and F) in the worms of indicated genotypes without (in black) or with (in red) the treatment of 100 μM $CuSO_4$. Data are displayed as box plots with each dot representing the data from each individual tested worm. Statistical significance of difference was analyzed by two-way ANOVA analysis with the post hoc test of Tukey's multiple comparison correction, and indicated as follows: ns = not significant, *$p < 0.05$, **$p < 0.01$, ***$p < 0.001$, ****$p < 0.0001$, and in different colors for varied comparisons. Black or red, a comparison of tested worms with the control (wild type N2, WT) under Cu^{2+}-untreated or Cu^{2+}-treated conditions; blue, that of Cu^{2+}-untreated with Cu^{2+}-treated worms of the same genotype.

(G) Curves (Left) and Hill plot (Right) of AIA axonal calcium responses to administration of $CuSO_4$ at various concentrations (in μM: 0, 0.01, 0.1, 1, 10, 50, 100, and 500). Data are presented as means ± SEM, as indicated by solid traces or dots ± gray shading or error bars, n ≥ 12. $\Delta F = F - F_0$. F, an average background signal-subtracted fluorescence intensity in an AIA axon in each frame (in gray shading); F_0, the average background signal-subtracted fluorescence intensity of an AIA axon within the initial 60 s before stimulation.

(H) Linear correlation of the egg-laying rates and the Cu^{2+}-elicited changes in the AIA axonal Ca^{2+} transients in WT worms treated with Cu^{2+} at various concentrations. Data on the egg-laying rates share with those in Figure 1B.

(I) Linear correlation of the Cu^{2+}-elicited changes in axonal Ca^{2+} transients in AIAs with the HSN Ca^{2+} signals in WT worms treated with Cu^{2+} at various concentrations (in μM: 0, 0.01, 0.1, 1, 10, 50, 100, and 500). Data on the HSN Ca^{2+} signals share with those in Figure 1F.

(J–M) Changes in the axonal Ca^{2+} signals evoked by 100 μM Cu^{2+} in AIA interneurons in WT, neuron blocked worms (J), *eat-4* mutant and its transgenetic worms (K), *glc-3* mutant and its transgenetic worms (L), and *eat-4*; *glc-3* mutant and its transgenetic worms (M). Data are displayed as box plots with each dot representing the data from each individual tested animal. Data are displayed as box plots with each dot representing the data from each individual tested animal. Statistical significance of difference was analyzed by one-way ANOVA with the post hoc test of Dunnett's multiple comparison correction compared with WT worms or as indicated, and denoted as follows: ns = not significant, **$p < 0.01$, ***$p < 0.001$, and ****$p < 0.0001$.

See also Figure S4–S6 and Table S1.

Given that ASIs reciprocally inhibit ASHs (Guo et al., 2015), the effects of ASI::*TeTx* are likely a result of the functional interaction between two sensory neurons.

Continual inhibition of neurotransmission by TeTx at embryonic periods may interfere with the development of the nervous system. Therefore, spatiotemporally optogenetic and chemogenetic manipulation of neurons is used favorably in neuroscience studies. We further employed chemogenetic activation of ASHs and ADLs as further evidence to support our results of TeTx manipulation. We expressed TRPV1 in ASHs and ADLs and employed capsaicin to excite tested neurons under standard culture conditions (Guo et al., 2015, 2018; Liu et al., 2019; Tobin et al., 2002). The chemogenetic activation of ADLs alone did not affect egg laying. In contrast, the activation of ASHs or both ASHs and ADLs (i.e., ASHs) and even TRPV1 expression *per se* in ASHs significantly inhibited spontaneous egg laying (Figure S4C). This result suggests that our chemogenetic activation of ASHs and ADLs was not strong enough to mimic Cu^{2+} stimulation, and the TRPV1 channel may have displayed leaky activity.

In summary, our results show that primary ASHs and secondary ADLs regulate egg laying and HSN activity differently. ASHs modulate egg laying and HSN activity under both standard culture conditions and Cu^{2+} treatments, while ADLs regulate both activities only under Cu^{2+} exposure. Thus, there may be two different glutamate effect sites or two receptors.

ASH/ADL, AIA, and HSN Disinhibitory Circuits Initiate Cu^{2+}-Induced Hyperactive Egg Laying

glc-3(*ok321*) mutants do not enhance egg laying in the presence of Cu^{2+} (Figures S2C and S2D). *glc-3* is expressed in many interneurons, including AIAs and AIYs, and motor neurons (Blazie et al., 2017; https://wormbase.org; Shinkai et al., 2011; Wenick and Hobert, 2004). AIAs are postsynaptic to ASHs and ADLs (Cook et al., 2019; https://www.wormatlas.org; White et al., 1986). Thus, GLC-3 signaling very likely mediates the regulation of egg laying by ASHs and ADLs under Cu^{2+} treatment. The GLC-3 protein is an L-glutamate-gated chloride channel subunit (Horoszok et al., 2001). This protein mediates the inhibition of AIAs by ASHs in the regulation of behavioral choice on stimulation of attractive diacetyl and noxious Cu^{2+} (Shinkai et al., 2011). We first used neuron::*TeTx* transgenes to screen *glc-3*-expressing interneurons that may function in egg-laying regulation. The AIA::*TeTx* transgene displayed maximal egg laying under standard culture conditions and exhibited no behavioral response to short-term Cu^{2+} treatment (Figures S4A and S4B). Therefore, we decided to focus on AIA neurons. We used *glc-3* mutant, *glc-3* genetically rescued worms, and AIA::*TeTx* transgene to further test AIA function in the regulation of HSN activity and egg laying. As expected, the AIA::*TeTx* transgene also displayed the same phenotype in HSN activity as egg laying (Figures 4A–4C). However, the *glc-3*(*ok321*) mutant did not phenocopy the AIA::*TeTx* transgene. The mutant displayed only hypoactive egg laying and HSN activity under Cu^{2+} treatments. The genetic rescue of *glc-3* in GLC-3-expressing cells (driven by *glc-3p*) or AIA alone (directed by *gcy-28*(*d*)*p*) but not in AIY interneurons (directed by *T19C4.5p* [Chalasani et al., 2007]) fully restored wild-type phenotypes

(Figures 4A–4C and S5A). This result indicated that GLC-3 signaling in AIAs may only regulate egg laying and HSN activity under Cu^{2+} treatment; however, AIAs *per se* regulate both activities in *C. elegans* under both states. AIAs may tonically inhibit egg laying in normal cultured worms. To test the regulatory function of the ASH/ADL and AIA circuits, we next used the *eat-4*(*ky5*); *glc-3*(*ok321*) double mutant and reconstituted *eat-4*, *glc-3,* and both genes in the mutant. Interestingly, *eat-4*(*ky5*); *glc-3*(*ok321*) fully phenocopied the AIA::*TeTx* transgene. Only the dual reconstitution of both *eat-4* in ASHs or ASHs/ADLs and *glc-3* in AIAs restored wild-type phenotypes in both Cu^{2+}-untreated and Cu^{2+}-treated worms. Dual reconstitution of *eat-4* in ADLs and *glc-3* in AIAs was enough to restore wild-type phenotypes in Cu^{2+}-treated but not in Cu^{2+}-untreated animals (Figures 4D–4F and S5B). The abovementioned results suggest that GLC-3 signaling in AIAs is involved in egg-laying regulation under Cu^{2+} treatments and that glutamate from ASHs modulates egg-laying and HSN activity under both states.

Both egg-laying rates and intensities of HSN Ca^{2+} transients displayed dose-dependent responses to Cu^{2+} stimuli, which were well fitted by the Hill function with EC_{50} = 4.68 μM and 2.46 μM, respectively (Figures 1B and 1F). Next, we examined the relation of AIA activities with Cu^{2+} doses using Ca^{2+} imaging combined with a microfluidic device. The Ca^{2+} transients in AIAs in wild-type N2 worms dose-dependently decreased upon treatment with Cu^{2+} at various concentrations. The Ca^{2+} responses were well fitted by the Hill function with a half-maximal inhibitory concentration (IC_{50}) = 2.28 μM (Figures 4G and S6A). Although the conditions for behavioral tests and Ca^{2+} imaging were different, the intensities of AIA Ca^{2+} transients negatively and linearly correlated with egg-laying rates and levels of HSN Ca^{2+} transients (Pearson r = −0.9689 and −0.9859, respectively, Figures 4H and 4I). We further examined AIA Ca^{2+} signals in response to Cu^{2+} challenge under genetic and neuronal manipulations as follows. Blocking neurotransmission by TeTx in ASHs, ADLs, and both types of neurons almost equally eliminated the inhibition of Cu^{2+}-induced Ca^{2+} transients in AIAs by both sensory neurons (Figures 4J and S6B). Loss-of-function mutation of *eat-4* or *glc-3* similarly augmented the AIA Ca^{2+} response to 100 μM Cu^{2+}. The *eat-4* reconstitution in ASHs, ADLs, or both neurons in *eat-4*(*ky5*) and *glc-3* in AIAs in *glc-3*(*ok321*) restored the wild-type phenotype (Figures 4K, 4L, and S6C). The *eat-4*; *glc-3* double mutant phenocopied with a single mutant of *eat-4* or *glc-3*. As expected, the dual rescue of *eat-4* in each type of sensory neuron and *glc-3* in AIAs, neither *eat-4* in ASHs nor ADLs nor *glc-3* in AIAs, restored wild-type Cu^{2+}-induced AIA Ca^{2+} signals (Figures 4M and S6D). The above results suggest that sensory ASH and ADL neurons release the neurotransmitter glutamate in a graded manner to inhibit AIA interneurons in response to Cu^{2+} stimulation. Thus, the removal of AIA inhibition (disinhibition) initiates Cu^{2+}-evoked hyperactive egg laying and HSN activity.

AIAs and HSNs chemosynaptically connect with each other (Cook et al., 2019; https://www.wormatlas.org; White et al., 1986). AIAs release acetylcholine, a classic neurotransmitter, and neuropeptides may include FLP-1, FLP-2, and INS-1 (Altun-Gultekin et al., 2001; Chalasani et al., 2010; Li and Kim, 2008). HSNs express two acetylcholine receptors: a non-alpha subunit ACR-14 and a G protein-linked receptor GAR-2 (https://wormbase.org; https://www.wormatlas.org; Rand, 2007). However, it is unknown whether HSNs express neuropeptide receptor(s). Therefore, we focused on acetylcholine signaling using mutants of acetylcholine biosynthesis and acetylcholine receptors. CHO-1 is the only high-affinity vesicular choline transporter in *C. elegans* (Matthies et al., 2006; Okuda et al., 2000). The *cho-1*(*tm373*) fully phenocopied the AIA::*TeTx* transgene phenotypes (Figures 5A–5C and S7A). Both strains displayed maximum egg-laying and HSN Ca^{2+} signals under standard culture conditions. The Cu^{2+} challenges did not further augment either activity. The genetic rescue of *cho-1* in all of its expression neurons and AIAs (with the *gcy-28*(*d*) promoter), not in other single types of *cho-1*-expressing neurons, fully restored wild-type phenotypes (Figures 5A–5C, S7A, and S8). These results indicate that AIAs inhibit HSN activity, suppress egg laying, and mediate Cu^{2+}-induced augmentation of egg laying via acetylcholine signaling.

An acetylcholine receptor mutant of *gar-2* showed a partial defect in the inhibition of egg laying (Bany et al., 2003). We next identified cholinergic receptor(s) that may be involved in the regulation of egg laying and HSN activity. Our results showed that the acetylcholine receptor ACR-14 mutant *acr-14*(*ok1155*) displayed similar phenotypes to those in *cho-1*(*tm373*), while *gar-2*(*ok520*) exhibited wild-type phenotypes (Figure S8). Genetically rescuing *acr-14* in all its expression neurons and HSNs (with *egl-6*(*a*) promoter) but not in other single types of *acr-14*-expressing neurons restored wild-type phenotypes (Figures 5D–5F, S7B, and S8). Moreover, the *cho-1*(*tm373*); *acr-14*(*ok1155*) double mutant exhibited very similar phenotypes to those in the single mutant of *cho-1*(*tm373*) or *acr-14*(*ok1155*), and the phenotypic defects were eliminated only by double genetic rescue of both *cho-1* in AIAs and *acr-14* in HSNs (Figures 5G–5I and

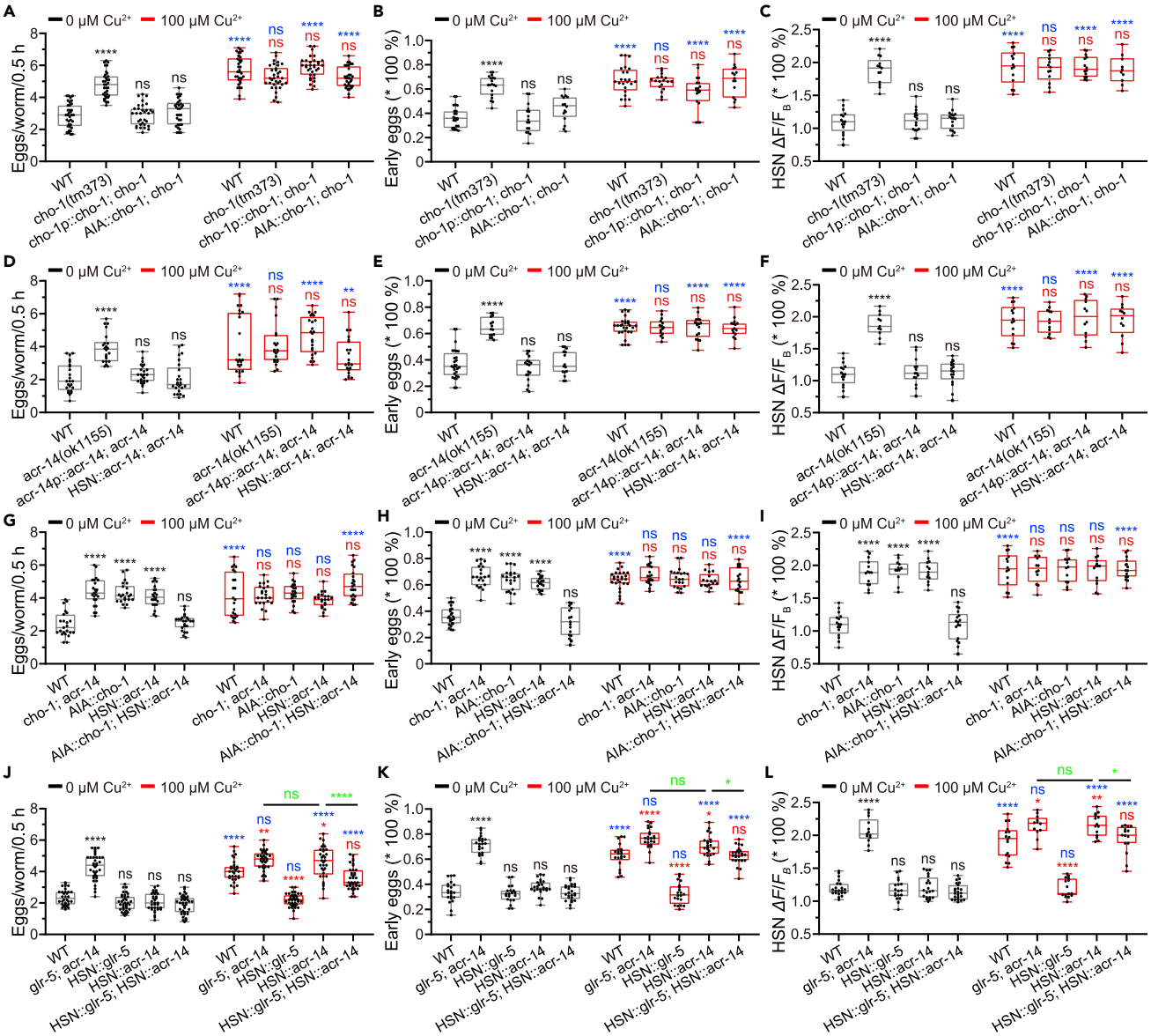

Figure 5. Acetylcholine Receptor ACR-14 Mediates AIA Inhibition on HSN Activity and Egg-Laying in Worms Treated without and with Cu^{2+}

(A–L) The number of the eggs laid per worm per 30 min (egg-laying rate, A, D, G, and J), percent of the eggs at early developmental stages (both 1–8 cells and 9–20 cells, B, E, H, and K) and HSN somal calcium signals (C, F, I, and L) in the worms of indicated genotypes treated without (in black) and with (in red) 100 μM $CuSO_4$. $\Delta F = F - F_B$. F, the average fluorescence intensity of the region of interest (ROI) of an HSN soma in each frame; F_B, a background signal defined as the average fluorescence intensity of ROI adjacent to the HSN soma in all frames.

All Data are displayed as box plots with each dot representing the data from each individual tested worm. Statistical significance of difference was analyzed by two-way ANOVA analysis with the post hoc test of Tukey's multiple comparison correction and indicated as follows: ns = not significant, *$p < 0.05$, **$p < 0.01$, ****$p < 0.0001$, and in different colors for varied comparisons. Black, a comparison of tested worms with the control (wild type N2 worm) under standard culture conditions; red, that of tested animals with the control under the Cu^{2+} exposure; blue, that of Cu^{2+}-untreated with Cu^{2+}-treated animals of the same genotype; green, that as indicated.

See also Figure S7, S8, and Table S1.

S7C). These results indicate that AIAs inhibit HSNs and thus inhibit egg laying via the acetylcholinergic ACR-14 receptor.

We further generated *glr-5*(*tm3506*); *acr-14*(*ok1155*) double mutants to test the functions of GLR-5 and ACR-14 signaling in regulating HSN activity and egg laying under different conditions. The *glr-5*; *acr-14*

double mutant differed in phenotypes from *cho-1*(*tm373*), *acr-14*(*ok1155*), and *cho-1*(*tm373*); *acr-14*(*ok1155*) mutants (Figure 5J–5L and S7D). The latter three mutants almost entirely phenocopied with each other. The *glr-5*; *acr-14* mutant displayed augmented but not maximal activities in egg-laying and HSNs under standard culture conditions. The Cu^{2+} treatments further increased both events. In genetically rescued transgenes, the reconstitution of either *glr-5* or *acr-14* alone or both genes in HSNs was enough to restore WT phenotypes under standard culture conditions. However, the dual rescue of both *glr-5* and *acr-14* in HSNs was necessary and sufficient to recover wild-type activities under Cu^{2+} treatments. Notably, HSN::*acr-14*; *glr-5*; *acr-14* transgenic worms displayed maximal responses of egg laying and HSN activity to Cu^{2+} treatments, as did *glr-5*; *acr-14* double mutant, while HSN::*glr-5*; *glr-5*; *acr-14* transgenic animals lost behavioral and cellular responses to Cu^{2+} stimulation (Figures 5J–5L and S7D).

The above results support the following conclusions. Under standard culture conditions, ASHs and AIAs inhibit both HSN activity and egg laying redundantly via the GLR-5 and ACR-14 signaling pathways. In contrast, upon Cu^{2+} exposure, ASHs release glutamate at high levels to inhibit HSNs and AIAs via GLR-5 and GLC-3 receptors. ADLs only act on AIAs via high-concentration glutamate and the GLC-3 receptor. Therefore, ASHs/ADLs remove AIA inhibition on egg laying and HSN activity. Thus, ASHs/ADLs, AIAs, and HSNs form a disinhibitory circuit. Disinhibition, a model of neurosignal integration, provides the basis for the function of this circuit.

Glutamatergic Receptors GLR-5 and GLC-3 with Distinct Sensitivities to Ligand Decode Intensities of Sensory Signals from ASHs and ADLs under Different Conditions

Our above results indicate that sensory ASH and ADL neurons modulate egg-laying behavior differently. ASHs downregulate and upregulate egg laying under standard culture conditions and Cu^{2+} exposure, respectively. In contrast, ADLs only regulate egg laying under Cu^{2+} exposure. Two glutamatergic receptors and two circuits are involved in the regulation of egg laying and HSN activity, specifically the GLR-5 and GLC-3 receptors, ASHs to HSNs inhibitory connection via GLR-5, and the disinhibitory circuitry consisting of ASHs/ADLs, AIAs, and HSNs. Previous studies report that two different receptors of a neurotransmitter decode the intensity of sensory signals and direct varied behaviors under different environmental conditions. Two glutamate receptors, GLR-1 and GLR-5, on AIB interneurons decode the intensity of sensory information and yield different behavioral outputs. GLR-1, exhibiting a low activation threshold (high sensitivity) and fast kinetics, functions in reversal initiation induced by quinine at low concentrations. GLR-5, which possesses a higher activation threshold (low sensitivity) and more sustained kinetics, acts in pumping inhibition by quinine at high levels (Zou et al., 2018). The octopaminergic receptors SER-3 and SER-6 (with high and low sensitivities; without direct evidence) function in two distinct neurons and circuits (Liu et al., 2019). These receptors augment pharyngeal pumping and maintain basal pumping and 5-HT production under the conditions of food supply and food deprivation (Liu et al., 2019).

The results of the present study show that the glutamatergic GLR-5 receptor functions to inhibit HSN activity and egg laying under standard culture conditions. Under this state, ASHs release low levels of glutamate. In contrast, the GLC-3 receptor primarily serves to inhibit AIA activity and augment HSN activity and egg laying under Cu^{2+} challenge that stimulates ASH and ADL sensory neurons to release high-level glutamate. Based on these results, it is reasonable to deduce that the two receptors may have different sensitivities to glutamate. GLR-5 and GLC-3 should be strongly and weakly sensitive, respectively. We subsequently used robust egg-laying and HSN activity assays to (indirectly) test this working hypothesis.

First, we challenged wild-type N2 animals with glutamate at various concentrations under standard culture conditions. Our results show that the egg-laying rates and HSN Ca^{2+} transients in WT worms dose-dependently increased in response to exogenous glutamate of different doses, which were accurately fitted by the Hill function with EC_{50} = 29.13 μM and 23.66 μM, respectively (Figures 6A, 6B, and S9A). The Hill responses suggest that there is only one glutamate effector, one glutaminergic receptor, or one functional site under this state. The egg-laying rates linearly correlated with HSN Ca^{2+} signals (Pearson r = 0.9818); however, we performed two tests under distinct conditions. In addition, in WT worms, the intensities of AIA Ca^{2+} transients dose-dependently decreased upon stimulation with glutamate at various concentrations (accurately fitted by the Hill function with IC_{50} = 23.53 μM, Figures 6C and S10A). The egg-laying rates and HSN Ca^{2+} signals negatively and linearly correlated with AIA Ca^{2+} signals (Pearson r = −0.9722 and −0.9962, respectively). Moreover, Ca^{2+} transients in AIAs decreased upon intensive chemogenetic activation of ASHs (with capsaicin at 1 μM, Figure S11).

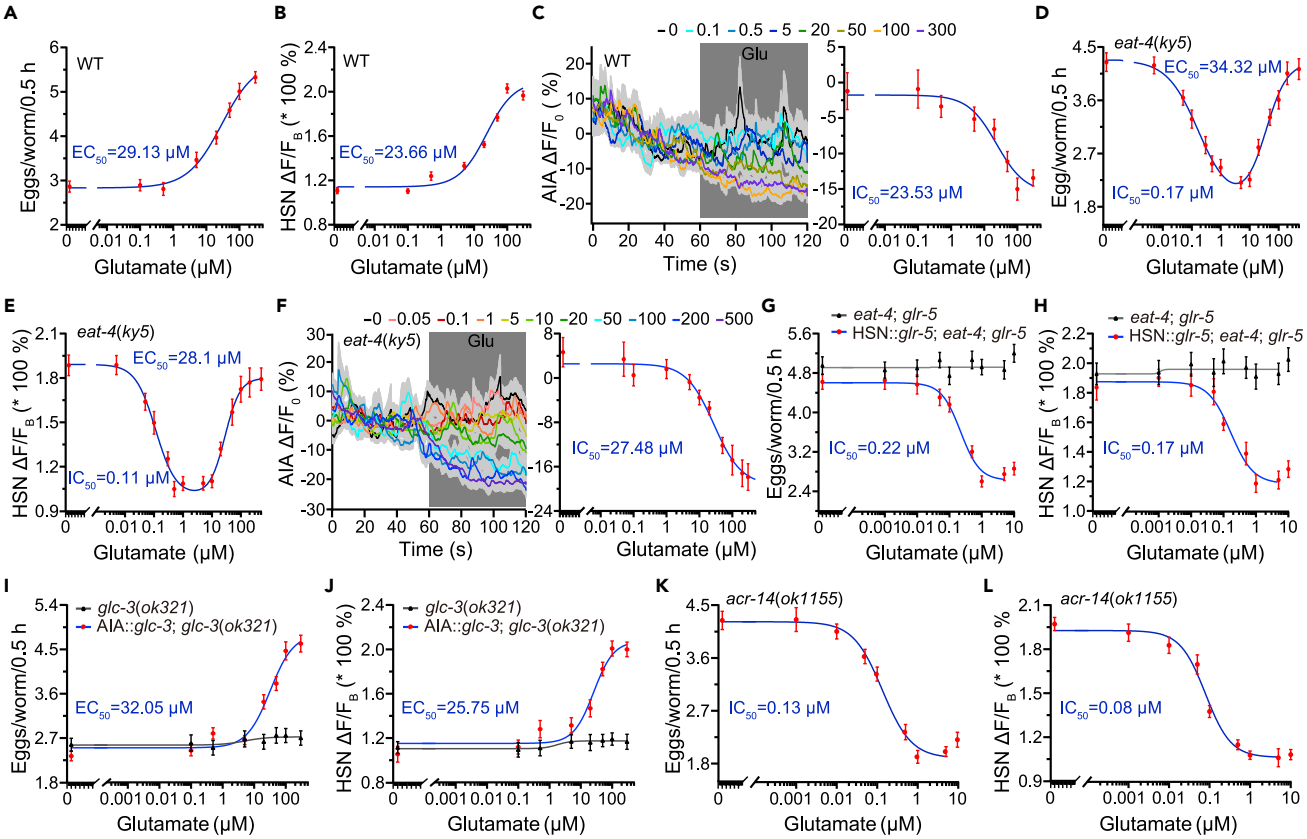

Figure 6. Bidirectional Regulation of Egg-Laying and HSN Activity in *C. elegans* by the Neurotransmitter Glutamate

(A and B) Hill plots of the egg-laying rates (A) and the HSN somal Ca^{2+} signals (B) in wild type N2 worms treated with exogenous glutamate at various concentrations (0, 0.1, 0.5, 5, 20, 50, 100, and 300, in μM).

(C) Curves and Hill plot of the AIA axonal Ca^{2+} signals in WT worms treated with exogenous glutamate at various concentrations (in μM: 0, 0.1, 0.5, 5, 20, 50, 100, and 300).

(D and E) Two-binding-sites Hill plots of the egg-laying rates (D) and the HSN somal Ca^{2+} signals (E) in *eat-4* mutant worms treated with exogenous glutamate at various concentrations (in μM: 0, 0.005, 0.05, 0.1, 0.3, 0.5, 1, 5, 10, 20, 50, 100, 200, and 500).

(F) Curves and Hill plot of the axonal AIA Ca^{2+} signals in *eat-4* mutant worms treated with exogenous glutamate at various concentrations (in μM: 0, 0.05, 0.1, 1, 5, 10, 20, 50, 100, 200, and 500).

(G and H) Hill plots of the egg-laying rates (G) and the HSN somal Ca^{2+} signals (H) in the indicated worms treated with exogenous glutamate at various concentrations (in μM: 0, 0.001, 0.01, 0.05, 0.1, 0.5, 1, 5, and 10).

(I and J) Hill plots of the egg-laying rates (I) and the HSN somal Ca^{2+} signals (J) in the indicated worms treated with exogenous glutamate at various concentrations (in μM: 0, 0.1, 0.5, 5, 20, 50, 100, and 300).

(K and L) Hill plots of the egg-laying rates (K) and the HSN somal Ca^{2+} signals (L) in *acr-14* mutant worms treated with exogenous glutamate at various concentrations (in μM: 0, 0.001, 0.01, 0.05, 0.1, 0.5, 1, 5, and 10).

All data are represented as means ± SEM, as indicated by dots or solid traces ± error bars or gray shading. See also Figures S9–S11 and Table S1.

Second, we used *eat-4*(*ky5*) to perform the same set of tests. Interestingly, in contrast to WT worms, the mutant displayed double-Hill responses of egg-laying rates (Figure 6D) and HSN Ca^{2+} signals (Figures 6E and S9B) to exogenous glutamate treatments, i.e., inhibitory and excitatory reactions in ranges of low and high concentrations, respectively. Two responses were well fitted by a two-binding-site Hill function with IC_{50} and EC_{50} values of 0.17 and 34.32 for egg-laying rates and 0.11 and 28.1 μM for the HSN Ca^{2+} transients, respectively, suggesting two effectors (two receptors or functional sites) of glutamate. The egg-laying rates linearly correlated with HSN Ca^{2+} signals (Pearson $r = 0.9835$). However, in this mutant, AIA Ca^{2+} signals were only well fitted by the single-binding-site Hill function, with IC_{50} = 27.48 μM (Figures 6F and S10B). Notably, the IC_{50} for AIA responses was close to the EC_{50} for HSN reactions (28.1 μM). The EC_{50} and IC_{50} values in the *eat-4* mutant worms were higher than those in WT worms. A reasonable explanation is that the glutamate levels in wild-type N2 animals under standard culture conditions should be a few micromolar (approximately 4.5 μM). AIA Ca^{2+} signals correlated negatively and linearly with egg-laying rates and HSN Ca^{2+} signals (Pearson $r = -0.9674$ and

−0.9838, respectively). The difference in the dependence on glutamate between WT worms and the *eat-4* mutant, combined with previous results, suggests that GLR-5 and GLC-3 not only function differently but are also distinctly sensitive to the neurotransmitter glutamate. GLR-5 is highly sensitive to glutamate and may be saturated by low-level glutamate, even under standard culture conditions, in wild-type N2 worms.

Third, we employed the *eat-4*; *glr-5* double mutant and transgenes to further evaluate the kinetics of GLR-5 and GLC-3 receptors indirectly, as we did previously. As expected, the double mutant lost the responses to glutamate challenges in egg laying and HSN Ca^{2+} signals. GLR-5 reconstitution in the HSN::*glr-5*; *eat-4*; *glr-5* transgene enabled worms to respond to glutamate with an inhibitory Hill relationship of IC_{50} = 0.22 μM and 0.17 μM for egg laying and HSN activity, respectively (Figures 6G and 6H). The IC_{50} values were comparable to those in the *eat-4* mutant (0.17 μM and 0.11 μM, Figures 6D and 6E). Two actions were linearly correlated (Pearson r = 0.9840) in this transgene.

Fourth, we reconstituted *glc-3* in the *glc-3*(*ok321*) mutant for the next test. This mutant also lost responses to glutamate treatments in egg-laying and HSN Ca^{2+} transients. GLC-3 expression in AIAs restored both reactions in the transgene. The EC_{50} values of Hill responses in egg laying and HSN activity were 32.05 μM and 25.75 μM, respectively, and comparable to those in N2 worms (29.13 μM and 23.66 μM, Figures 6A and 6B). Two reactions linearly correlated (Pearson r = 0.9844) in this transgene (Figures 6I and 6J, and S9D).

Fifth, as shown in Figures 6K, 6L and S9E, the *acr-14*(*ok1155*) mutant displayed sole inhibitory Hill responses to glutamate treatments, with IC_{50} values of 0.13 and 0.08 μM for egg-laying rates and HSN Ca^{2+} responses, respectively, which were also linearly correlated (Pearson r = 0.982). Interestingly, among *eat-4*(*ky5*), HSN::*glr-5*; *eat-4*; *glr-5* and *acr-14*(*ok1155*) worms, the *acr-14* mutant possessed the lowest IC_{50} values, suggesting that AIAs may inhibit HSNs and egg laying tonically.

In summary, our experiments suggest that glutamatergic receptors GLR-5 and GLC-3 have different affinities to glutamate, although biochemical tests for binding kinetics are still needed. The apparent IC_{50} and EC_{50} values of these receptors to glutamate are approximately 0.1 μM and 30 μM (estimated by an indirect method), respectively. The sensitivity difference of the two receptors enables decoding the intensities of sensory signals glutamate and translating them into different behavioral outputs through a single neurotransmitter.

DISCUSSION

In *C. elegans*, egg-laying behavior is among the best-characterized behaviors and has been used not only for behavioral studies but also for the genetic analysis of nervous system function and development (Schafer, 2005, 2006; Zhang et al., 2008). Worms maintain a relatively constant number of unlaid eggs in the uterus (McCarter et al., 1999). Egg laying occurs through the contraction of vulval muscles. Electrically coupled vm2s, which are the only egg-laying muscles receiving significant synaptic input from two HSN and six VC motor neurons (Cook et al., 2019; White et al., 1986), are essential for opening the vulva (Schafer, 2006). Most egg laying occurs in short bursts lasting approximately 1–2 min, which represents an active phase. A more extended quiescent period averaging approximately 20 min in duration separates the active phases (Collins et al., 2016; Collins and Koelle, 2013; Schafer, 2005, 2006; Trent et al., 1983; Waggoner et al., 1998; Weinshenker et al., 1995). Serotonin, released primarily from the HSNs and, to a lesser extent, from VC4 and VC5, facilitates the onset of the active phase, while HSNs and VCs release acetylcholine to trigger individual muscle contractions within the active phase (Waggoner et al., 1998). HSN neurons release serotonin and the neuropeptide NLP-3, which act as partially redundant co-transmitters to initiate egg laying (Brewer et al., 2019). HSNs are postsynaptic to sensory neurons (ASHs, ASIs, ASJs, AIMs, and PLMs), interneurons (AIAs, AIYs, AVBs, AVFs, AVJs, BDUs, PVQs, PVNs, RIFs, and RIR), and VC motor neurons (Cook et al., 2019; https://www.wormatlas.org; White et al., 1986). HSNs also receive humoral regulation from vulval muscle cells in modulating the development of the two-state patterned activity, i.e., alternate active and quiescent periods (Ravi et al., 2018; Schafer, 2005, 2006). Sensory information from the touch receptor ALM and PLM neurons (Zhang et al., 2008), chemosensory ASIs, ASJs (Liu et al., 2018), and AWCs (Fenk and de Bono, 2015) inhibits HSN activity and egg laying. The results of this study help to elucidate the regulation of egg laying by environmental stress.

In the present study, we found that short-term noxious exposure to metal ions, such as Cu^{2+}, Ni^{2+}, Mn^{2+}, and Fe^{3+}, evokes hyperactive egg laying in *C. elegans*. We have dissected the molecular and neurocircuit mechanisms underlying ASH and ADL modulation of HSN activity and egg laying under varied environmental conditions. Our results suggest a working model in which sensory ASH and ADL neurons sense Cu^{2+} stimulation

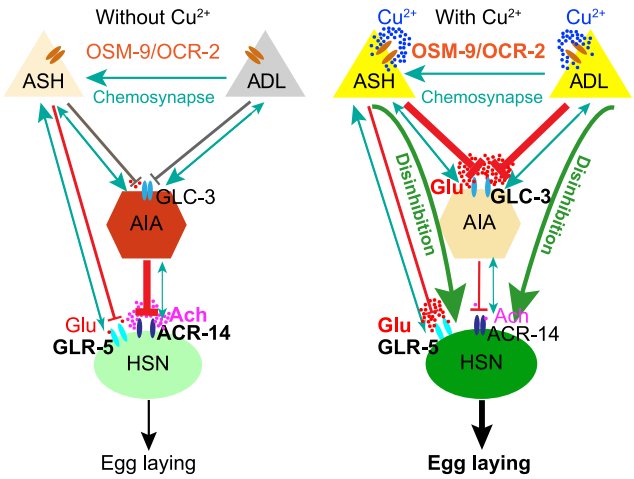

Figure 7. The Molecular and Neurocircuital Mechanisms Underlying the Opposite Modulation of Egg-Laying under Standard Culture Conditions and Exposure to Cu^{2+} in *C. elegans*

Under standard culture conditions, sensory neuron ASHs tonically release a small amount of glutamate (red dots) to inhibit (red line) HSN motor neurons via GLR-5 signaling. In contrast, AIA interneurons release high-level acetylcholine (magenta dots) to suppress HSNs via ACR-14 signaling. Under noxious stimulation of Cu^{2+} (blue dots), ASHs and ADLs release a large amount of glutamate to inhibit AIAs via GLC-3 signaling and thus remove (green lines with arrows) HSN depression by AIAs (disinhibition). ASHs, but not ADLs (no chemosynaptic connection with HSNs), suppress activity in HSNs via GLR-5 receptor under the Cu^{2+} challenge. However, the action of disinhibitory ASH/ADL-AIA-HSN predominates over ASH inhibition on HSNs. The azure arrows indicate chemosynapses. The width of arrows and lines shows the intensities of synapses and actions, including inhibition and excitation. The different colors indicate the power of cellular activity and actions: undertone and deep colors, weak and robust activities, respectively; gray, no evident activity or action.

through OCR-2/OSM-9 signaling (Figure 7). Under standard culture conditions, ASHs tonically release a small amount of neurotransmitter glutamate to inhibit HSN activity and egg-laying behavior via GLR-5 signaling in HSNs. Under Cu^{2+} treatment, ASHs and ADLs release a large amount of glutamate to regulate egg laying via two circuits: the ASH-HSN inhibitory circuit via the highly sensitive GLR-5 receptor and the disinhibitory ASH/ADL-AIA-HSN circuit. In the latter circuitry, ASHs and ADLs release high levels of glutamate and thus inhibit AIA interneurons via the low sensitivity of the GLC-3 receptor, consequently relieving AIA inhibition on HSNs via ACR-14 signaling. This circuitry predominates over the former circuitry in this activity (Figure 7). Our study indirectly supports that the graded release of neurotransmitter glutamate encodes sensory signals from ASHs and ADLs. Two receptors, GLR-5 and GLC-3, with distinct sensitivities to ligands, encode sensory signals and induce different behavioral outputs under varied environmental conditions.

Copper (Cu) is an essential element for animals and plants; however, increased uptake caused deleterious effects in the normal functioning of organisms, with a narrow difference amid the indispensable and detrimental concentrations. The typical values of Cu in uncontaminated soils varied from 2 to 109 mg kg^{-1}. The human industrial and agricultural activities, including mining, refinery, fossil fuel combustion, waste incineration, traffic, fertilizers, and soil amendments, cause copper contamination in the environment (Kumar et al., 2020; Malhotra et al., 2020). Exposure of even low-level Cu (down to 0.05 μg/L) caused a hatching delay in Zebrafish *Brachydanio rerio* (Dave and Xiu, 1991). The long-term exposure of excessive Cu decreases successful hatching and suppresses the development of eggs in pulmonate snail, *Physa acuta* (Gao et al., 2017), and reduces *C. elegans* brood size and lead to internal hatching of offspring inside their mothers (bagging) (Calafato et al., 2008). High level of Cu deteriorates hatching success and hatched juvenile survival in antarctic terrestrial nematode *Plectus murrayi* (Brown et al., 2020). Here, we find that short-term Cu exposure augments egg laying in *C. elegans*. This observation argues for the life-history theory, which argues that when organisms experience environmental conditions that can reduce their long-term reproductive success, they increase their present reproductive output.

AIA interneurons inhibit HSN activity and egg laying. Nociceptive ASHs and ADLs inhibit AIA activity under noxious exposure to Cu^{2+} ions (this study). AIAs are first-layer amphid interneurons; they are postsynaptic to

12 cells: sensory ASK, ASH, ASG, ADL, ASE, AWC, and ASI; and they form gap junctions with ASI, AWA, and ADF neurons (https://www.wormatlas.org). AIAs integrate information from amphid sensory neurons and regulate multiple behaviors. The ablation of AIAs shortens the duration of forward locomotion (Gray et al., 2005; Tsalik and Hobert, 2003; Wakabayashi et al., 2004). AIAs control foraging behavior (Calhoun et al., 2015; Lopez-Cruz et al., 2019). These neurons integrate sensory information of pathogen *P. aeruginosa* from ASHs/ASIs and mediate avoidance and immune response to the pathogen (Cao et al., 2017). AIAs integrate signals from ASK (via inhibitory synapses) and other sensory neurons and play essential roles in attraction to pheromone ascarosides and innate social behavior (Macosko et al., 2009; Srinivasan et al., 2012). AIAs receive excitatory and inhibitory inputs from AWAs and ASHs/ADLs (via GLC-3 signaling), respectively, and regulate the behavioral choice between conflicting alternatives when worms are facing conflicting sensory cues, such as diacetyl and Cu^{2+} (Shinkai et al., 2011). AIAs receive excitatory inputs from ASER and provide feedback to ASER to generate chemotaxis learning (Tomioka et al., 2006). However, AIAs are unlikely to be essential for egg-laying suppression by 5% CO_2 (Fenk and de Bono, 2015).

The results of the present study indicate that AIAs inhibit HSN activity and egg-laying behavior via acetylcholine/ACR-14 signaling. Based on the synaptic connections and functions of AIA interneurons, we suggest that AIAs function as a primary hub for integrating multiple sensory cues to modulate egg laying. ACR-14, a non-α subunit of the ACR-16 group, is categorized by homologs (Jones and Sattelle, 2004; Mongan et al., 1998; Nassel, 2018); however, to the best of our knowledge, ACR-14 is not involved in nicotine responses in *C. elegans*, including nicotine approach (Sellings et al., 2013), withdrawal, and sensitization (Feng et al., 2006). The signal transduction pathway employed by ACR-14 warrants further study.

Sensory signal encoding, decoding, and behavioral translation are fundamental issues in neuroscience. The nervous system encodes environmental stimuli through the type (vision, audition, taste, smell, balance, touch, proprioception, temperature sense, pain, or itch) and the quality (spatial, position, intensity, or frequency) of a stimulus. Sensory neurons may release different types of neurotransmitters or graded amounts of a neurotransmitter in response to different stimulation conditions to encode sensory signals (see reviews by Burnstock, 2004; Nassel, 2018; Nusbaum et al., 2017). The receptors of neurotransmitters or neuromodulators decode sensory cues, and neural circuits integrate neuroinformation and then translate it into behavioral outputs.

In *C. elegans*, different neurotransmitter receptors decode sensory information from polymodal ASH sensory neurons and drive different avoidant behaviors (Hart et al., 1995; Maricq et al., 1995). Moreover, distinct receptors of a single neurotransmitter decode sensory intensity encoding by the amount of a single neurotransmitter. For instance, both glutamatergic NMDA (NMR-1) and non-NMDA (GLR-1 and GLR-2) receptor subunits mediate the osmotic avoidance response, while non-NMDA receptors mediate the response to mechanical stimuli (Mellem et al., 2002). The neuromodulator serotonin acts directly on vulval muscles via $G_q\alpha$ signaling to increase the frequency of Ca^{2+} transients and worm egg-laying rate. However, serotonin inhibits spontaneous activity in HSNs via $G_o\alpha$ signaling (Shyn et al., 2003). Two glutamate receptors, GLR-1 and GLR-5, encode sensory signals of quinine at different concentrations. GLR-1 is highly sensitive and is rapidly inactivated; in contrast, GLR-5 is less sensitive and is slowly inactivated. These two receptors on AIB interneurons decode low and high concentrations of quinine and translate into reversal initiation and feeding suppression, respectively (Zou et al., 2018). SER-3 and SER-6, strongly and weakly sensitive receptors, possibly decode varied neuroinformation (graded octopamine release) from Ring interneuron (RICs) under food supply and food deprivation. SER-3 responds to octopamine at low levels to augment pharyngeal pumping via an ADF–RIC–SIA feedforward circuit under abundant supply. SER-6 mainly works at high levels of octopamine via a disexcitatory ADF-RIC-AWB-ADF feedback circuit to maintain basal pumping and serotonin production in ADFs under food deprivation (Liu et al., 2019).

In this study, we indirectly detected that the graded release of neurotransmitter glutamate encodes sensory information from ASHs and ADLs. Highly sensitive GLR-5 receptors on HSNs decode low-intensity sensory signals from ASHs under standard culture conditions. These receptors translate neuronal information into the inhibition of egg laying by directly inhibiting HSN activity. However, low-sensitivity GLC-3 receptors on AIAs decode high-intensity signals from ASHs and ADLs under noxious Cu^{2+} administration and translate neuroinformation into behavioral augmentation by subtracting AIA suppression on HSNs. At the same time, ASHs still inhibit HSNs directly. Using behavioral assays, Ca^{2+} imaging, and pharmacological tests, we indirectly estimated the apparent dose-dependent IC_{50} and EC_{50} of the two receptors. GLR-5 and GLC-3 are strongly and weakly sensitive to glutamate, respectively.

Limitations of the Study

The results in the study support that varied amounts of neurotransmitter glutamate are released under different conditions, and two glutamatergic receptors have different sensitivities to the neurotransmitter. However, direct measurement of neurotransmitters released and assays of the binding kinetics of receptors with the ligand are required to support the conclusions directly.

Resource Availability

Lead Contact

Further information and requests for resources and reagents should be directed to and will be fulfilled by the Lead Contact, Zheng-Xing Wu (ibbwuzx@mail.hust.edu.cn).

Materials Availability

All worm strains and plasmids used in this study are available to scientist's community. Please email the Lead Contact.

Data and Code Availability

The published article includes all data generated or analyzed during this study.

METHODS

All methods can be found in the accompanying Transparent Methods supplemental file.

SUPPLEMENTAL INFORMATION

Supplemental Information can be found online at https://doi.org/10.1016/j.isci.2020.101588.

ACKNOWLEDGMENTS

We thank the Caenorhabditis Genetic Center (CGC) and National BioResource Project (NBRP) for the worm strains used in this study, Dr. B.F. Liu for the support of fabrication of microfluidic devices, and Dr. J. Yao for rat TRPV1 cDNA. This work was supported by the grants from the National Science Foundation of China (31471034) and the Fundamental Research Funds for the Central Universities (2016YXZD062).

AUTHOR CONTRIBUTIONS

Z.X.W. supervised the study; X.W., Y.H.C., and R.L. performed the major part of the experiments, analyzed the data, and created the figures, M.H.G., S.W.Y., J.J.W., J.H.H., H.L. and P.Z.W. performed the minor part of the experiments; X.W., E.G., and Z.X.W. wrote the paper. All authors participated in discussions and data interpretation.

DECLARATION OF INTERESTS

The authors declare no competing interests.

Received: May 6, 2020
Revised: August 7, 2020
Accepted: September 16, 2020
Published: October 23, 2020

REFERENCES

Adamo, S.A. (1999). Evidence for adaptive changes in egg laying in crickets exposed to bacteria and parasites. Anim. Behav. *57*, 117–124.

Alkema, M.J., Hunter-Ensor, M., Ringstad, N., and Horvitz, H.R. (2005). Tyramine functions independently of octopamine in the *Caenorhabditis elegans* nervous system. Neuron *46*, 247–260.

Allendorf, F.W., and Hard, J.J. (2009). Human-induced evolution caused by unnatural selection through harvest of wild animals. Proc. Natl. Acad. Sci. U S A *106* (*Suppl 1*), 9987–9994.

Altun-Gultekin, Z., Andachi, Y., Tsalik, E.L., Pilgrim, D., Kohara, Y., and Hobert, O. (2001). A regulatory cascade of three homeobox genes, *ceh-10, ttx-3* and *ceh-23*, controls cell fate specification of a defined interneuron class in *C. elegans*. Development *128*, 1951–1969.

Bany, I.A., Dong, M.Q., and Koelle, M.R. (2003). Genetic and cellular basis for acetylcholine inhibition of *Caenorhabditis elegans* egg-laying behavior. J. Neurosci. *23*, 8060–8069.

Bargmann, C.I. (2006). Chemosensation in *C. elegans*. WormBook, 1-29. http://www.wormbook.org/chapters/www_chemosensation/chemosensation.html.

Bargmann, C.I., Thomas, J.H., and Horvitz, H.R. (1990). Chemosensory cell function in the behavior and development of *Caenorhabditis elegans*. Cold Spring Harb. Symp. Quant. Biol. *55*, 529–538.

Baskett, M.L., and Barnett, L.A.K. (2015). The ecological and evolutionary consequences of marine reserves. Annu. Rev. Ecol. Evol. Syst. *46*, 150807173404008.

Bellocchio, E.E., Reimer, R.J., Fremeau, R.T., Jr., and Edwards, R.H. (2000). Uptake of glutamate into synaptic vesicles by an inorganic phosphate transporter. Science *289*, 957–960.

Blazie, S.M., Geissel, H.C., Wilky, H., Joshi, R., Newbern, J., and Mangone, M. (2017). Alternative polyadenylation directs tissue-specific miRNA targeting in *Caenorhabditis elegans* somatic tissues. Genetics *206*, 757–774.

Brown, K.E., Wasley, J., and King, C.K. (2020). Sensitivity to copper and development of culturing and toxicity test procedures for the antarctic terrestrial nematode *Plectus murrayi*. Environ. Toxicol. Chem. *39*, 482–491.

Brewer, J.C., Olson, A.C., Collins, K.M., and Koelle, M.R. (2019). Serotonin and neuropeptides are both released by the HSN command neuron to initiate *Caenorhabditis elegans* egg laying. PLoS Genet. *15*, e1007896.

Brockie, P.J., Madsen, D.M., Zheng, Y., Mellem, J., and Maricq, A.V. (2001). Differential expression of glutamate receptor subunits in the nervous system of *Caenorhabditis elegans* and their regulation by the homeodomain protein UNC-42. J. Neurosci. *21*, 1510–1522.

Brockie, P.J., and Maricq, A.V. (2003). Ionotropic glutamate receptors in *Caenorhabditis elegans*. Neurosignals *12*, 108–125.

Burnstock, G. (2004). Cotransmission. Curr. Opin. Pharmacol. *4*, 47–52.

Calafato, S., Swain, S., Hughes, S., Kille, P., and Sturzenbaum, S.R. (2008). Knock down of *Caenorhabditis elegans cutc-1* exacerbates the sensitivity toward high levels of copper. Toxicol. Sci. *106*, 384–391.

Calhoun, A.J., Tong, A., Pokala, N., Fitzpatrick, J.A., Sharpee, T.O., and Chalasani, S.H. (2015). Neural mechanisms for evaluating environmental variability in *Caenorhabditis elegans*. Neuron *86*, 428–441.

Cao, X., Kajino-Sakamoto, R., Doss, A., and Aballay, A. (2017). Distinct roles of sensory neurons in mediating pathogen avoidance and neuropeptide-dependent immune regulation. Cell Rep. *21*, 1442–1451.

Chalasani, S.H., Kato, S., Albrecht, D.R., Nakagawa, T., Abbott, L.F., and Bargmann, C.I. (2010). Neuropeptide feedback modifies odor-evoked dynamics in *Caenorhabditis elegans* olfactory neurons. Nat. Neurosci. *13*, 615–621.

Chalasani, S.H., Chronis, N., Tsunozaki, M., Gray, J.M., Ramot, D., Goodman, M.B., and Bargmann, C.I. (2007). Dissecting a circuit for olfactory behaviour in *Caenorhabditis elegans*. Nature *450*, 63–70.

Choi, S., Taylor, K.P., Chatzigeorgiou, M., Hu, Z., Schafer, W.R., and Kaplan, J.M. (2015). Sensory neurons arouse *C. elegans* locomotion via both glutamate and neuropeptide Release. PLoS Genet. *11*, e1005359.

Clark, D.A., Gabel, C.V., Lee, T.M., and Samuel, A.D. (2007). Short-term adaptation and temporal processing in the cryophilic response of *Caenorhabditis elegans*. J. Neurophysiol. *97*, 1903–1910.

Collins, K.M., Bode, A., Fernandez, R.W., Tanis, J.E., Brewer, J.C., Creamer, M.S., and Koelle, M.R. (2016). Activity of the *C. elegans* egg-laying behavior circuit is controlled by competing activation and feedback inhibition. Elife *5*, e21126.

Collins, K.M., and Koelle, M.R. (2013). Postsynaptic ERG potassium channels limit muscle excitability to allow distinct egg-laying behavior states in *Caenorhabditis elegans*. J. Neurosci. *33*, 761–775.

Cook, S.J., Jarrell, T.A., Brittin, C.A., Wang, Y., Bloniarz, A.E., Yakovlev, M.A., Nguyen, K.C.Q., Tang, L.T.H., Bayer, E.A., Duerr, J.S., et al. (2019). Whole-animal connectomes of both *Caenorhabditis elegans* sexes. Nature *571*, 63–71.

Dave, G., and Xiu, R.Q. (1991). Toxicity of mercury, copper, nickel, lead, and cobalt to embryos and larvae of zebrafish, *Brachydanio rerio*. Arch. Environ. Contam. Toxicol. *21*, 126–134.

Davis, M.W., Morton, J.J., Carroll, D., and Jorgensen, E.M. (2008). Gene activation using FLP recombinase in *C. elegans*. Plos Genet. *4*, e1000028.

de Bono, M., and Maricq, A.V. (2005). Neuronal substrates of complex behaviors in *C. elegans*. Annu. Rev. Neurosci. *28*, 451–501.

Dempsey, C.M., Mackenzie, S.M., Gargus, A., Blanco, G., and Sze, J.Y. (2005). Serotonin (5HT), fluoxetine, imipramine and dopamine target distinct 5HT receptor signaling to modulate *Caenorhabditis elegans* egg-laying behavior. Genetics *169*, 1425–1436.

Desai, C., and Horvitz, H.R. (1989). *Caenorhabditis elegans* mutants defective in the functioning of the motor neurons responsible for egg laying. Genetics *121*, 703–721.

Dingle, H. (1990). The evolution of life histories. In Population Biology, K. Wöhrmann, ed. (Springer), pp. 267–289.

Duerr, J.S., Gaskin, J., and Rand, J.B. (2001). Identified neurons in *C. elegans* coexpress vesicular transporters for acetylcholine and monoamines. Am. J. Physiol. Cell Physiol. *280*, C1616–C1622.

Eikeset, A.M., Dunlop, E.S., Heino, M., Storvik, G., Stenseth, N.C., and Dieckmann, U. (2016). Roles of density-dependent growth and life history evolution in accounting for fisheries-induced trait changes. Proc. Natl. Acad. Sci. U S A *113*, 15030–15035.

Emtage, L., Aziz-Zaman, S., Padovan-Merhar, O., Horvitz, H.R., Fang-Yen, C., and Ringstad, N. (2012). IRK-1 potassium channels mediate peptidergic inhibition of *Caenorhabditis elegans* serotonin neurons via a G_o signaling pathway. J. Neurosci. *32*, 16285–16295.

Feng, Z., Li, W., Ward, A., Piggott, B.J., Larkspur, E.R., Sternberg, P.W., and Xu, X.Z. (2006). A *C. elegans* model of nicotine-dependent behavior: regulation by TRP-family channels. Cell *127*, 621–633.

Fenk, L.A., and de Bono, M. (2015). Environmental CO_2 inhibits *Caenorhabditis elegans* egg-laying by modulating olfactory neurons and evokes widespread changes in neural activity. Proc. Natl. Acad. Sci. U S A *112*, E3525–E3534.

Fox, R.J., Fromhage, L., and Jennions, M.D. (2019). Sexual selection, phenotypic plasticity and female reproductive output. Philos. Trans. R. Soc. Lond. B Biol. Sci. *374*, 20180184.

Gao, L., Doan, H., Nidumolu, B., Kumar, A., and Gonzago, D. (2017). Effects of copper on the survival, hatching, and reproduction of a pulmonate snail (*Physa acuta*). Chemosphere *185*, 1208–1216.

Gray, J.M., Hill, J.J., and Bargmann, C.I. (2005). A circuit for navigation in *Caenorhabditis elegans*. Proc. Natl. Acad. Sci. U S A *102*, 3184–3191.

Greenwald, I.S., and Horvitz, H.R. (1982). Dominant suppressors of a muscle mutant define an essential gene of *Caenorhabditis elegans*. Genetics *101*, 211–225.

Guo, J., Martin, P.R., Zhang, C., and Zhang, J.E. (2017). Predation risk affects growth and reproduction of an invasive snail and its lethal effect depends on prey size. PLoS One *12*, e0187747.

Guo, M., Ge, M., Berberoglu, M.A., Zhou, J., Ma, L., Yang, J., Dong, Q., Feng, Y., Wu, Z., and Dong, Z. (2018). Dissecting molecular and circuit mechanisms for inhibition and delayed response of ASI. Neurons during nociceptive stimulus. Cell Rep. *25*, 1885–1897.e9.

Guo, M., Wu, T.H., Song, Y.X., Ge, M.H., Su, C.M., Niu, W.P., Li, L.L., Xu, Z.J., Ge, C.L., Al-Mhanawi, M.T.H., et al. (2015). Reciprocal inhibition between sensory ASH and ASI neurons modulates nociception and avoidance in *Caenorhabditis elegans*. Nat. Commun. *6*, e5655.

Hart, A.C., Sims, S., and Kaplan, J.M. (1995). Synaptic code for sensory modalities revealed by *C. elegans* GLR-1 glutamate receptor. Nature *378*, 82–85.

Heino, M., Pauli, B.D., and Dieckmann, U. (2015). Fisheries-induced evolution. Annu. Rev. Ecol. Evol. Syst. *46*, 461–480.

Hilliard, M.A., Apicella, A.J., Kerr, R., Suzuki, H., Bazzicalupo, P., and Schafer, W.R. (2005). In vivo imaging of *C. elegans* ASH neurons: cellular response and adaptation to chemical repellents. EMBO J. *24*, 63–72.

Hilliard, M.A., Bargmann, C.I., and Bazzicalupo, P. (2002). *C. elegans* responds to chemical repellents by integrating sensory inputs from the head and the tail. Curr. Biol. *12*, 730–734.

Hills, T., Brockie, P.J., and Maricq, A.V. (2004). Dopamine and glutamate control area-restricted search behavior in *Caenorhabditis elegans*. J. Neurosci. *24*, 1217–1225.

Hirshfield, M.F., and Tinkle, D.W. (1975). Natural selection and the evolution of reproductive effort. Proc. Natl. Acad. Sci. U S A *72*, 2227–2231.

Hobson, R.J., Hapiak, V.M., Xiao, H., Buehrer, K.L., Komuniecki, P.R., and Komuniecki, R.W. (2006). SER-7, a *Caenorhabditis elegans* 5-HT7-like receptor, is essential for the 5-HT stimulation of pharyngeal pumping and egg laying. Genetics *172*, 159–169.

Horoszok, L., Raymond, V., Sattelle, D.B., and Wolstenholme, A.J. (2001). GLC-3: a novel fipronil and BIDN-sensitive, but picrotoxinin-insensitive, L-glutamate-gated chloride channel subunit from *Caenorhabditis elegans*. Br. J. Pharmacol. *132*, 1247–1254.

Jones, A.K., and Sattelle, D.B. (2004). Functional genomics of the nicotinic acetylcholine receptor gene family of the nematode, *Caenorhabditis elegans*. Bioessays *26*, 39–49.

Kahn-Kirby, A.H., and Bargmann, C.I. (2006). TRP channels in *C. elegans*. Annu. Rev. Physiol. *68*, 719–736.

Kaplan, J.M., and Horvitz, H.R. (1993). A dual mechanosensory and chemosensory neuron in *Caenorhabditis elegans*. Proc. Natl. Acad. Sci. U S A *90*, 2227–2231.

Kavanagh, P.S., and Kahl, B.L. (2016). Life history theory. In Encyclopedia of Evolutionary Psychological Science, V. Weekes-Shackelford, T.K. Shackelford, and V.A. Weekes-Shackelford, eds. (Cham: Springer International Publishing), pp. 1–12.

Killeen, A., and Marin de Evsikova, C. (2016). Effects of sub-lethal teratogen exposure during larval development on egg laying and egg quality in adult *Caenorhabditis Elegans*. F1000Res *5*, 2925.

Kim, K., and Li, C. (2004). Expression and regulation of an FMRFamide-related neuropeptide gene family in *Caenorhabditis elegans*. J. Comp. Neurol. *475*, 540–550.

Kumar, V., Pandita, S., Singh Sidhu, G.P., Sharma, A., Khanna, K., Kaur, P., Bali, A.S., and Setia, R. (2020). Copper bioavailability, uptake, toxicity and tolerance in plants: a comprehensive review. Chemosphere *262*, 127810.

Lee, R.Y., Sawin, E.R., Chalfie, M., Horvitz, H.R., and Avery, L. (1999). EAT-4, a homolog of a mammalian sodium-dependent inorganic phosphate cotransporter, is necessary for glutamatergic neurotransmission in *Caenorhabditis elegans*. J. Neurosci. *19*, 159–167, http://www.wormbook.org/chapters/www_neuropeptides/neuropeptides.html.

Li, C., and Kim, K. (2008). Neuropeptides. WormBook, pp. 1–36, http://www.wormbook.org/chapters/www_neuropeptides/neuropeptides.html.

Liu, H., Qin, L.W., Li, R., Zhang, C., Al-Sheikh, U., and Wu, Z.X. (2019). Reciprocal modulation of 5-HT and octopamine regulates pumping via feedforward and feedback circuits in *C. elegans*. Proc. Natl. Acad. Sci. U S A *116*, 7107–7112.

Liu, Z., Kariya, M.J., Chute, C.D., Pribadi, A.K., Leinwand, S.G., Tong, A., Curran, K.P., Bose, N., Schroeder, F.C., Srinivasan, J., et al. (2018). Predator-secreted sulfolipids induce defensive responses in *C. elegans*. Nat. Commun. *9*, 1128.

Lopez-Cruz, A., Sordillo, A., Pokala, N., Liu, Q., McGrath, P.T., and Bargmann, C.I. (2019). Parallel multimodal circuits control an innate foraging behavior. Neuron *102*, 407–419.e8.

Macosko, E.Z., Pokala, N., Feinberg, E.H., Chalasani, S.H., Butcher, R.A., Clardy, J., and Bargmann, C.I. (2009). A hub-and-spoke circuit drives pheromone attraction and social behaviour in *C. elegans*. Nature *458*, 1171–1175.

Malhotra, N., Ger, T.R., Uapipatanakul, B., Huang, J.C., Chen, K.H., and Hsiao, C.D. (2020). Review of copper and copper nanoparticle toxicity in fish. Nanomaterials (Basel) *10*, 1126.

Maricq, A.V., Peckol, E., Driscoll, M., and Bargmann, C.I. (1995). Mechanosensory signalling in *C. elegans* mediated by the GLR-1 glutamate receptor. Nature *378*, 78–81.

Matthies, D.S., Fleming, P.A., Wilkes, D.M., and Blakely, R.D. (2006). The *Caenorhabditis elegans* choline transporter CHO-1 sustains acetylcholine synthesis and motor function in an activity-dependent manner. J. Neurosci. *26*, 6200–6212.

McCarter, J., Bartlett, B., Dang, T., and Schedl, T. (1999). On the control of oocyte meiotic maturation and ovulation in *Caenorhabditis elegans*. Dev. Biol. *205*, 111–128.

Mellem, J.E., Brockie, P.J., Zheng, Y., Madsen, D.M., and Maricq, A.V. (2002). Decoding of polymodal sensory stimuli by postsynaptic glutamate receptors in *C. elegans*. Neuron *36*, 933–944.

Mongan, N.P., Baylis, H.A., Adcock, C., Smith, G.R., Sansom, M.S., and Sattelle, D.B. (1998). An extensive and diverse gene family of nicotinic acetylcholine receptor alpha subunits in *Caenorhabditis elegans*. Receptor Channel *6*, 213–228.

Nassel, D.R. (2018). Substrates for neuronal co-transmission with neuropeptides and small molecule neurotransmitters in *Drosophila*. Front. Cell Neurosci. *12*, 83.

Nathoo, A.N., Moeller, R.A., Westlund, B.A., and Hart, A.C. (2001). Identification of neuropeptide-like protein gene families in *Caenorhabditis elegans* and other species. Proc. Natl. Acad. Sci. U S A *98*, 14000–14005.

Neil, B., and Ford, R.A.S. (1989). Phenotypic plasticity in reproductive traits evidence from a viviparous snake. Ecology *70*, 1768–1774.

Nusbaum, M.P., Blitz, D.M., and Marder, E. (2017). Functional consequences of neuropeptide and small-molecule co-transmission. Nat. Rev. Neurosci. *18*, 389–403.

Okuda, T., Haga, T., Kanai, Y., Endou, H., Ishihara, T., and Katsura, I. (2000). Identification and characterization of the high-affinity choline transporter. Nat. Neurosci. *3*, 120–125.

Polak, M., and Starmer, W.T. (1998). Parasite-induced risk of mortality elevates reproductive effort in male *Drosophila*. Proc. Biol. Sci. *265*, 2197–2201, http://www.wormbook.org/chapters/www_acetylcholine/acetylcholine.html.

Rand, J.B. (2007). Acetylcholine. WormBook, pp. 1–21, http://www.wormbook.org/chapters/www_acetylcholine/acetylcholine.html.

Rankin, C.H., and Wicks, S.R. (2000). Mutations of the *Caenorhabditis elegans* brain-specific inorganic phosphate transporter eat-4 affect habituation of the tap-withdrawal response without affecting the response itself. J. Neurosci. *20*, 4337–4344.

Ravi, B., Garcia, J., and Collins, K.M. (2018). Homeostatic feedback modulates the development of two-state patterned activity in a model serotonin motor circuit in *Caenorhabditis elegans*. J. Neurosci. *38*, 6283–6298.

Ringstad, N., and Horvitz, H.R. (2008). FMRFamide neuropeptides and acetylcholine synergistically inhibit egg-laying by *C. elegans*. Nat. Neurosci. *11*, 1168–1176.

Sambongi, Y., Nagae, T., Liu, Y., Yoshimizu, T., Takeda, K., Wada, Y., and Futai, M. (1999). Sensing of cadmium and copper ions by externally exposed ADL, ASE, and ASH neurons elicits avoidance response in *Caenorhabditis elegans*. Neuroreport *10*, 753–757.

Sawin, E.R. (1996). Genetic and cellular analysis of modulated behaviors in *C. elegans* (Department of Biology (Massachusetts Institute of Technology)).

Schafer, W.F. (2006). Genetics of egg-laying in worms. Annu. Rev. Genet. *40*, 487–509, http://www.wormbook.org/chapters/www_egglaying/egglaying.html.

Schafer, W.R. (2005). Egg-laying (WormBook), pp. 1–7, http://www.wormbook.org/chapters/www_egglaying/egglaying.html.

Schiavo, G., Benfenati, F., Poulain, B., Rossetto, O., Polverino de Laureto, P., DasGupta, B.R., and Montecucco, C. (1992). Tetanus and botulinum-B neurotoxins block neurotransmitter release by proteolytic cleavage of synaptobrevin. Nature *359*, 832–835.

Sellings, L., Pereira, S., Qian, C., Dixon-McDougall, T., Nowak, C., Zhao, B., Tyndale, R.F., and van der Kooy, D. (2013). Nicotine-motivated behavior in *Caenorhabditis elegans* requires the nicotinic acetylcholine receptor subunits *acr-5* and *acr-15*. Eur. J. Neurosci. *37*, 743–756.

Shinkai, Y., Yamamoto, Y., Fujiwara, M., Tabata, T., Murayama, T., Hirotsu, T., Ikeda, D.D., Tsunozaki, M., Iino, Y., Bargmann, C.I., et al. (2011). Behavioral choice between conflicting alternatives is regulated by a receptor guanylyl cyclase, GCY-28, and a receptor tyrosine kinase, SCD-2, in AIA interneurons of *Caenorhabditis elegans*. J. Neurosci. *31*, 3007–3015.

Shyn, S.I., Kerr, R., and Schafer, W.R. (2003). Serotonin and Go modulate functional states of neurons and muscles controlling *C. elegans* egg-laying behavior. Curr. Biol. *13*, 1910–1915.

Srinivasan, J., von Reuss, S.H., Bose, N., Zaslaver, A., Mahanti, P., Ho, M.C., O'Doherty, O.G., Edison, A.S., Sternberg, P.W., and Schroeder, F.C. (2012). A modular library of small molecule signals regulates social behaviors in *Caenorhabditis elegans*. Plos Biol. *10*, e1001237.

Teshiba, E., Miyahara, K., and Takeya, H. (2016). Glucose-induced abnormal egg-laying rate in *Caenorhabditis elegans*. Biosci. Biotechnol. Biochem. *80*, 1436–1439.

Therkildsen, N.O., Wilder, A.P., Conover, D.O., Munch, S.B., Baumann, H., and Palumbi, S.R. (2019). Contrasting genomic shifts underlie parallel phenotypic evolution in response to fishing. Science *365*, 487–490.

Tobin, D.M., Madsen, D.M., Kahn-Kirby, A., Peckol, E.L., Moulder, G., Barstead, R., Maricq, A.V., and Bargmann, C.I. (2002). Combinatorial expression of TRPV channel proteins defines their sensory functions and subcellular localization in *C. elegans* neurons. Neuron *35*, 307–318.

Tomioka, M., Adachi, T., Suzuki, H., Kunitomo, H., Schafer, W.R., and Iino, Y. (2006). The insulin/PI 3-kinase pathway regulates salt chemotaxis learning in *Caenorhabditis elegans*. Neuron *51*, 613–625.

Trent, C. (1983). Genetic and Behavioral Studies of the Egg-Laying System in *Caenorhabditis elegans* (Massachusetts Institute of Technology).

Trent, C., Tsuing, N., and Horvitz, H.R. (1983). Egg-laying defective mutants of the nematode *Caenorhabditis elegans*. Genetics *104*, 619–647.

Troemel, E.R., Chou, J.H., Dwyer, N.D., Colbert, H.A., and Bargmann, C.I. (1995). Divergent seven transmembrane receptors are candidate chemosensory receptors in *C. elegans*. Cell *83*, 207–218.

Tsalik, E.L., and Hobert, O. (2003). Functional mapping of neurons that control locomotory behavior in *Caenorhabditis elegans*. J. Neurobiol. *56*, 178–197.

Vezilier, J., Nicot, A., Gandon, S., and Rivero, A. (2015). Plasmodium infection brings forward mosquito oviposition. Biol. Lett. *11*, 20140840.

Voutev, R., and Hubbard, E.J. (2008). A "FLP-Out" system for controlled gene expression in *Caenorhabditis elegans*. Genetics *180*, 103–119.

Waggoner, L.E., Zhou, G.T., Schafer, R.W., and Schafer, W.R. (1998). Control of alternative behavioral states by serotonin in *Caenorhabditis elegans*. Neuron *21*, 203–214.

Wakabayashi, T., Kitagawa, I., and Shingai, R. (2004). Neurons regulating the duration of forward locomotion in *Caenorhabditis elegans*. Neurosci. Res. *50*, 103–111.

Wang, W., Qin, L.W., Wu, T.H., Ge, C.L., Wu, Y.Q., Zhang, Q., Song, Y.X., Chen, Y.H., Ge, M.H., Wu, J.J., et al. (2016). cGMP signalling mediates water sensation (hydrosensation) and hydrotaxis in *Caenorhabditis elegans*. Sci. Rep. *6*, 19779.

Wang, W., Xu, Z.J., Wu, Y.Q., Qin, L.W., Li, Z.Y., and Wu, Z.X. (2015). Off-response in ASH neurons evoked by $CuSO_4$ requires the TRP channel OSM-9 in *Caenorhabditis elegans*. Biochem. Biophys. Res. Commun. *461*, 463–468.

Weinshenker, D., Garriga, G., and Thomas, J.H. (1995). Genetic and pharmacological analysis of neurotransmitters controlling egg laying in *C. elegans*. J. Neurosci. *15*, 6975–6985.

Wenick, A.S., and Hobert, O. (2004). Genomic cis-regulatory architecture and trans-acting regulators of a single interneuron-specific gene battery in *C. elegans*. Dev. Cell *6*, 757–770.

White, J.G., Southgate, E., Thomson, J.N., and Brenner, S. (1986). The structure of the nervous system of the nematode *Caenorhabditis elegans*. Philos. Trans. R. Soc. Lond. B Biol. Sci. *314*, 1–340.

Whittaker, A.J., and Sternberg, P.W. (2004). Sensory processing by neural circuits in *Caenorhabditis elegans*. Curr. Opin. Neurobiol. *14*, 450–456.

Zhang, M., Chung, S.H., Fang-Yen, C., Craig, C., Kerr, R.A., Suzuki, H., Samuel, A.D., Mazur, E., and Schafer, W.R. (2008). A self-regulating feed-forward circuit controlling *C. elegans* egg-laying behavior. Curr. Biol. *18*, 1445–1455.

Zhang, M., Schafer, W.R., and Breitling, R. (2010). A circuit model of the temporal pattern generator of *Caenorhabditis* egg-laying behavior. BMC. Syst. Biol. *4*, 81.

Zou, W., Fu, J., Zhang, H., Du, K., Huang, W., Yu, J., Li, S., Fan, Y., Baylis, H.A., Gao, S., et al. (2018). Decoding the intensity of sensory input by two glutamate receptors in one *C. elegans* interneuron. Nat. Commun. *9*, 4311, http://www.wormbook.org/chapters/www_chemosensation/chemosensation.html.

iScience, Volume *23*

Supplemental Information

Signal Decoding for Glutamate Modulating Egg Laying Oppositely in *Caenorhabditis elegans* under Varied Environmental Conditions

Xin Wen, Yuan-Hua Chen, Rong Li, Ming-Hai Ge, Sheng-Wu Yin, Jing-Jing Wu, Jia-Hao Huang, Hui Liu, Ping-Zhou Wang, Einav Gross, and Zheng-Xing Wu

Supplemental Figures

Supplemental Figure 1

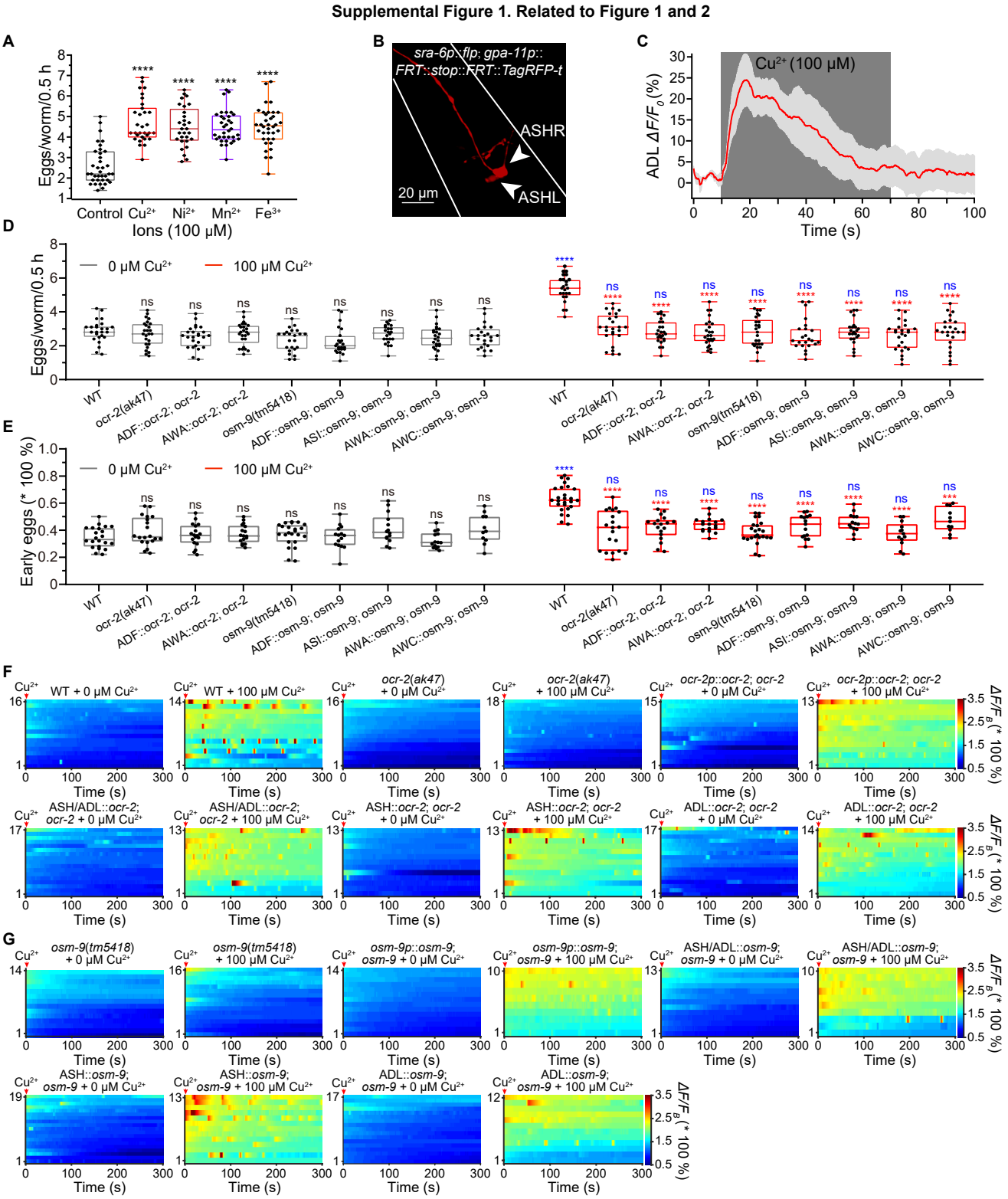

Figure S1. Acute and short-term treatments of copper ion (Cu^{2+}) excited HSN motor neurons and augmented egg-laying via sensation mediated by OCR-2/OSM-9 channel complex in sensory ASH and ADL neurons, respectively. Related to Figures 1 and 2.

(A) Short term (30 min) exposure of 100 μM metal ions, Cu^{2+} ($CuSO_4$), Ni^{2+} ($NiCl_2$), Mn^{2+} ($MnCl_2$) and Fe^{3+} ($Fe_2(SO_4)_3$), caused hyperactive egg-laying in wild type N2 (WT) worm as indicated by egg-laying rate. Data were displayed as box plots, with each dot representing the data from each individual tested animal. Statistical significance of difference was analyzed by one-way Analysis of Variance (ANOVA) with the post hoc test of Dunnett's multiple comparisons correction, ****$P < 0.0001$.

(B) The curve of Ca^{2+} signals in ADLs in WT worms treated with exogenous 100 μM Cu^{2+} (n=19). We performed the test using fluorescence imaging combined with a microfluidic device. Please see "Transparent Methods" for detail. Data were expressed as the means ± SEM, as indicated by solid red traces ± grey shading. $\Delta F = F - F_0$. F, an averaged fluorescence intensity of the region of interest (ROI) of ADL soma in each frame that is subtracted average background signal; F_0, that within 10 s before the Cu^{2+} stimulation.

(C) ASHs-specific gene expression driven by FLP-out system with intersectional promoters *sra-6p* and *gpa-11p*.

(D and E) Phenotypes of egg-laying in WT, mutant, and transgenic worms. The number of the eggs laid per worm for 30 min (egg-laying rate, D) and percent of the eggs at early developmental stages (stages of 1–8 cells and 9–20 cells, E) in WT (as a control), mutant and transgenic worms of indicated genotypes treated without (in black) or with (in red) 100 μM $CuSO_4$, respectively. The tested worms displayed no obvious defect in egg-laying phenotype without the Cu^{2+} administration, while they exhibited a significant defect in egg-laying under 30 min's treatment of 100 μM Cu^{2+}. The genotypes of transgenic worms are as follows: ADF::*ocr-2*; *ocr-2*(*ak47*), AWA::*ocr-2*; *ocr-2*(*ak47*), ADF::*osm-9*; *osm-9*(*tm5418*), ASI::*osm-9*; *osm-9*(*tm5418*), AWA::*osm-9*; *osm-9*(*tm5418*) and AWC::*osm-9*; *osm-9*(*tm5418*), respectively. Data were displayed as box plots with each dot representing the data from each individual tested worm. Statistical significance of difference was analyzed by two-way ANOVA analysis with the post hoc test of Tukey's multiple comparison correction and indicated as ns = not significant, *** $P < 0.001$, **** $P < 0.0001$, and in different colors for varied comparisons. Black or red, a comparison of tested worms with control under Cu^{2+}-untreated or Cu^{2+}-treated condition; blue, that of Cu^{2+}-untreated with Cu^{2+}-treated worms of the same genotype.

(F and G) Heat maps of percent changes in calcium transients in the soma of paired HSN motor neurons WT (as a control), mutant and transgenic worms of indicated genotype, respectively. Red arrows indicated the beginning time of the application of $CuSO_4$ (Cu^{2+}) solutions at concentrations indicated. $\Delta F = F - F_B$. F, an averaged fluorescence intensity of the region of interest (ROI) of an HSN soma in each frame; F_B, a background signal defined as the average fluorescence intensity of an ROI adjacent to the HSN soma in all frames. The label on the left y-axis indicates the number of tested worms. The genotypes of transgenic worms are as follows: *ocr-2p*::*ocr-2*; *ocr-2*(*ak47*), ASH/ADL::*ocr-2*; *ocr-2*(*ak47*), ASH::*ocr-2*; *ocr-2*(*ak47*), ADL::*ocr-2*; *ocr-2*(*ak47*), *osm-9p*::*osm-9*; *osm-9*(*tm5418*), ASH/ADL::*osm-9*; *osm-9*(*tm5418*), ASH::*osm-9*; *osm-9*(*tm5418*) and ADL::*osm-9*; *osm-9*(*tm5418*), respectively.

Supplemental Figure 2

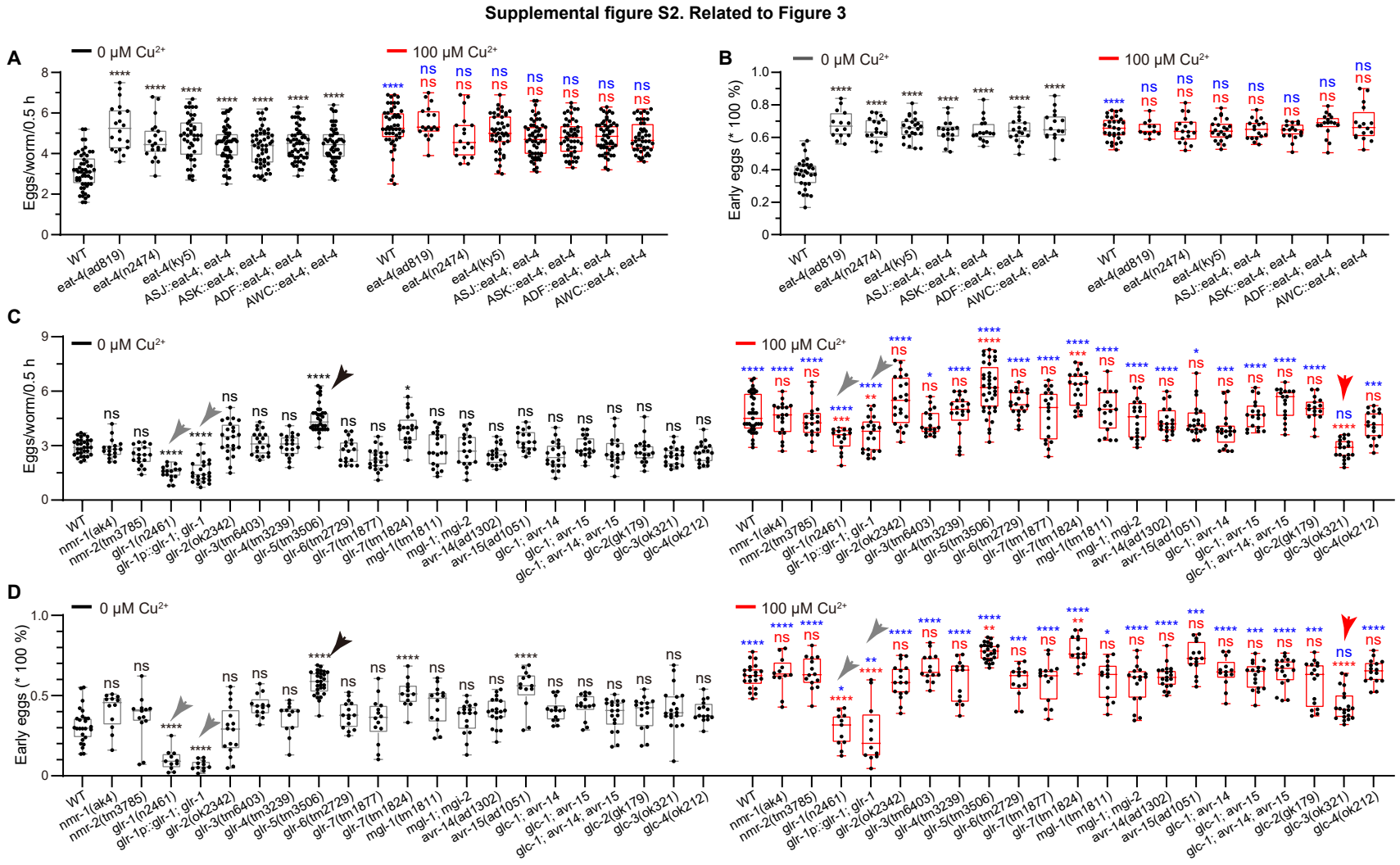

Figure S2. Screening glutamatergic neurons and genes encoding glutamate receptors to test whether they involve in egg-laying under the standard culture conditions and short-term noxious Cu^{2+} treatment. Related to figure 3.

(A and B) Phenotypes of egg-laying in wild type N2 (WT, as a control), *eat-4* mutant, and neuron-specific *eat-4* transgene worms. The number of the eggs laid per worm for 30 min (egg-laying rate, A) and percent of the eggs at early developmental stages (1–8 cells and 9–20 cells, B) in WT, mutant and transgenic worms without (in black) or with (in red) the treatment of 100 μM $CuSO_4$, respectively. The genotypes of transgenic worms are as follows: ASJ::*eat-4*; *eat-4*(*ky5*), ASK::*eat-4*; *eat-4*(*ky5*), ADF::*eat-4*; *eat-4*(*ky5*) and AWC::*eat-4*; *eat-4*(*ky5*), respectively.

(C and D) Phenotypes of egg-laying in WT and mutants of glutamatergic receptors. The egg-laying rate (C) and percent of the eggs at the early developmental stages (D) in WT and mutants without (in black) or with (in red) the treatment of 100 μM $CuSO_4$, respectively. Grey arrows indicate that *glr-1*(*n2461*) may have a defect in egg-laying behavior, but genetically rescuing driven by the promoter of the gene was not able to restore wild-type behavioral phenotype. Black arrows indicate that *glr-5*(*tm3506*) only displayed a defect in egg-laying without Cu^{2+} treatment. Red arrows indicate *glc-3*(*ok321*) only exhibited defect in egg-laying under treatment of 100 μM Cu^{2+}. The genotypes of double and triple mutant worms are as follows: *glc-1*(*pk54*); *avr-14*(*ad1302*), *glc-1*(*pk54*); *avr-15* (*ad1051*), *glc-1*(*pk54*); *avr-14*(*ad1302*); *avr-15*(*ad1051*), respectively.

All data were displayed as box plots with each dot representing the data from each individual tested worm. Statistical significance of difference was analyzed by two-way ANOVA analysis with the post hoc test of Tukey's multiple comparison correction. The *P*-value was indicated as follows: ns = not significant, * $P < 0.05$, ** $P < 0.01$, *** $P < 0.001$, **** $P < 0.0001$, and in different colors for varied comparisons. Black or red, a comparison of tested worms with control under Cu^{2+}-untreated or Cu^{2+}-treated condition; blue, that of Cu^{2+}-untreated with Cu^{2+}-treated worms of the same genotype.

Supplemental Figure 3

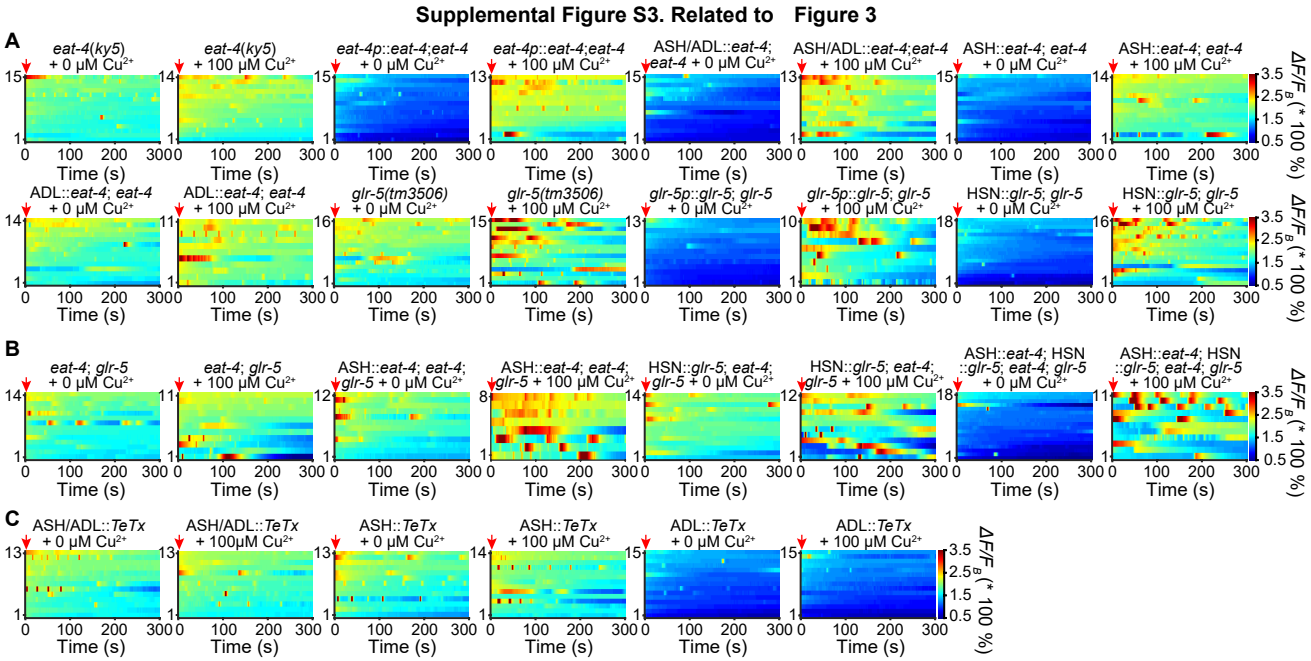

Figure S3. Changes in somal calcium transients in HSN motor neurons suggest that neurotransmitter released by ASH and ADL sensory neurons and GLR-5 signaling in HSNs involve in the modulation of egg-laying. Related to figure 3.

(A–C) Heat maps of percent changes in somal Ca^{2+} transients of HSN motor neurons in the worms of indicated genotypes treated without or with 100 μM $CuSO_4$, respectively. Red arrows indicated the beginning time of the application of $CuSO_4$ (Cu^{2+}) solutions at concentrations indicated. $\Delta F = F - F_B$. F, an averaged fluorescence intensity of the region of interest (ROI) of an HSN soma in each frame; F_B, a background signal defined as the average fluorescence intensity of an ROI adjacent to the HSN soma in all frames. The label on the left y-axis indicates the number of tested worms.

The genotypes of mutants and transgenic worms are as follows: *eat-4*(*ky5*), *eat-4p*::*eat-4*; *eat-4*(*ky5*), ASH/ADL::*eat-4*; *eat-4*(*ky5*), ASH::*eat-4*; *eat-4*(*ky5*), ADL::*eat-4*; *eat-4*(*ky5*), *glr-5*(tm3506), *glr-5p*::*glr-5*; *glr-5*(tm3506), HSN::*glr-5*; *glr-5*(tm3506), *eat-4*(*ky5*); *glr-5*(tm3506), ASH::*eat-4*; *eat-4*(*ky5*); *glr-5*(tm3506), HSN::*glr-5*; *eat-4*(*ky5*); *glr-5*(tm3506), ASH::*eat-4*; HSN::*glr-5*; *eat-4*(*ky5*); *glr-5*(tm3506), ASH/ADL::*TeTx*, ASH::*TeTx* and ADL::*TeTx*, respectively.

Supplemental Figure 4

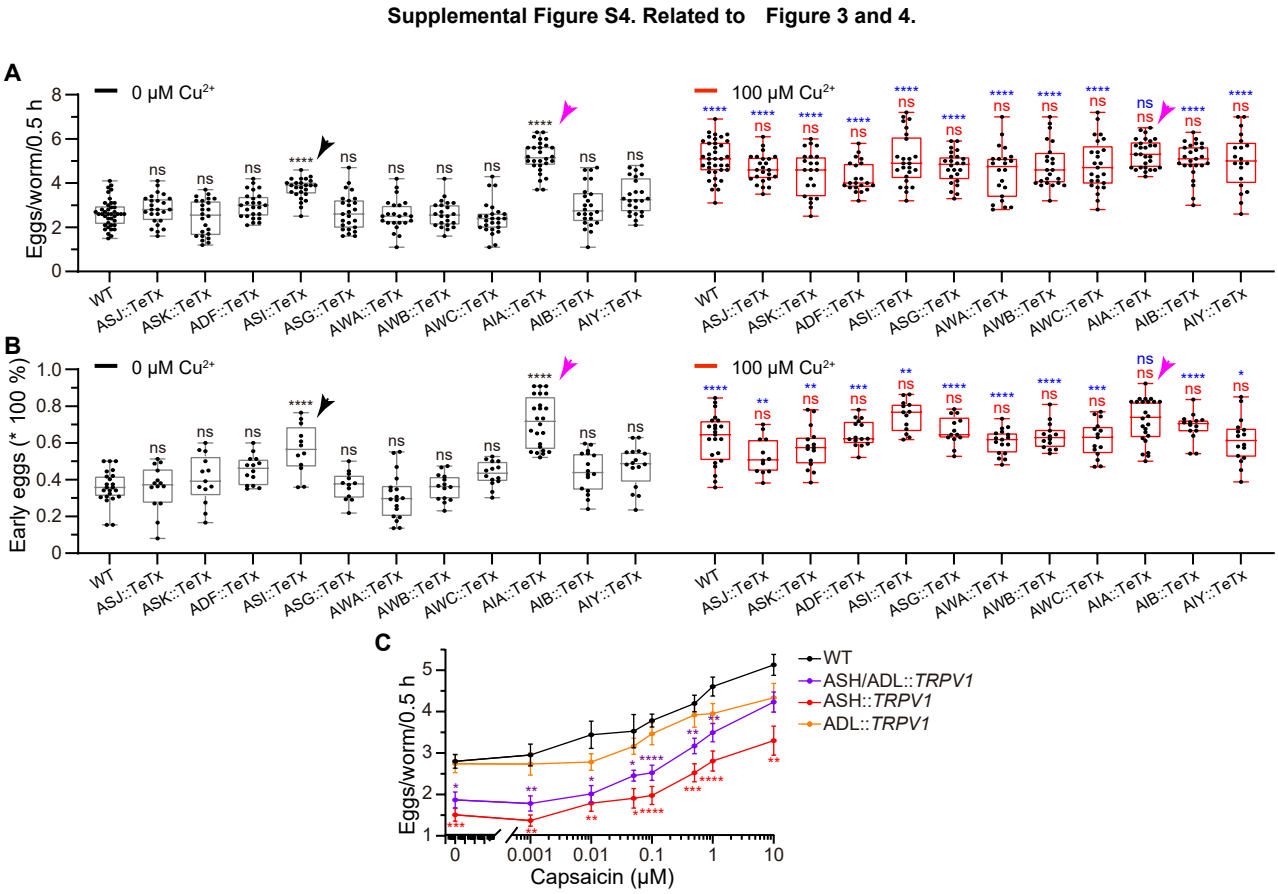

Figure S4. Egg-laying rate and percent of the eggs at early development stages under standard culture and Cu^{2+}-treatment in the transgenic and ASH chemogenetically activated worms. Related to figure 3 and 4.

(A and B) Phenotypes of egg-laying in wild type N2 (WT, as a control) and genetically neurotransmission-blocked worms (neuron-specific *TeTx* transgenes). The number of the eggs laid per animal per 30 min (egg-laying rate, A) and percent of the eggs at early developmental stages (1–8 cell and 9–20 cell, B) in WT and transgenic worms of indicated genotype without (in black) and with (in red) the treatment of 100 μM $CuSO_4$, respectively. Black arrows indicate that ASI::*TeTx* transgenic worm only displayed a defect in egg-laying without Cu^{2+} treatment. Magenta arrows show that the worms of indicated genotypes (AIA::*TeTx*) showed a defect in egg-laying under both un-exposure and exposure of 100 μM $CuSO_4$, judged by the significant differences in the egg-laying rate and percent of eggs at the early development stages. Data were displayed as box plots with each dot representing the data from each individual tested worm. Statistical significance of difference was analyzed by two-way ANOVA analysis with post hoc Tukey's multiple comparison correction tests. The *P*-value was indicated as follows: ns = not significant, * $P < 0.05$, ** $P < 0.01$, *** $P < 0.001$, **** $P < 0.0001$, and in different colors for varied comparisons. Black or red, a comparison of tested

worms with control under Cu^{2+}-untreated or Cu^{2+}-treated condition; blue, that of Cu^{2+}-untreated with Cu^{2+}-treated worms of the same genotype.

(C) The egg-laying rate in ASH, ASH/ADL, and ADL chemogenetically activated worms without Cu^{2+} treatment. Capsaicin at concentration at μM of 0, 0.001, 0.01, 0.05, 0.1, 0.5, 1 and 10, was used to activate TRPV1 channel. Except ADL activated worms, ASH/ADL, and ASH activated worms displayed significantly inhibited egg-laying even without capsaicin. Data were displayed as means ± SEM. Statistical significance of difference was analyzed by mixed-effects analysis with the post hoc test of Dunnett's multiple comparison correction compared with those in WT worms. The *P*-value was indicated as follows: in ADL::*TRPV1* transgenic worms, not significant (not indicated) at all cases; in ASH/ADL::*TRPV1* transgenic worms, ns = not significant (not indicated), * $P < 0.05$, ** $P < 0.01$, *** $P < 0.001$, **** $P < 0.0001$.

Supplemental Figure 5

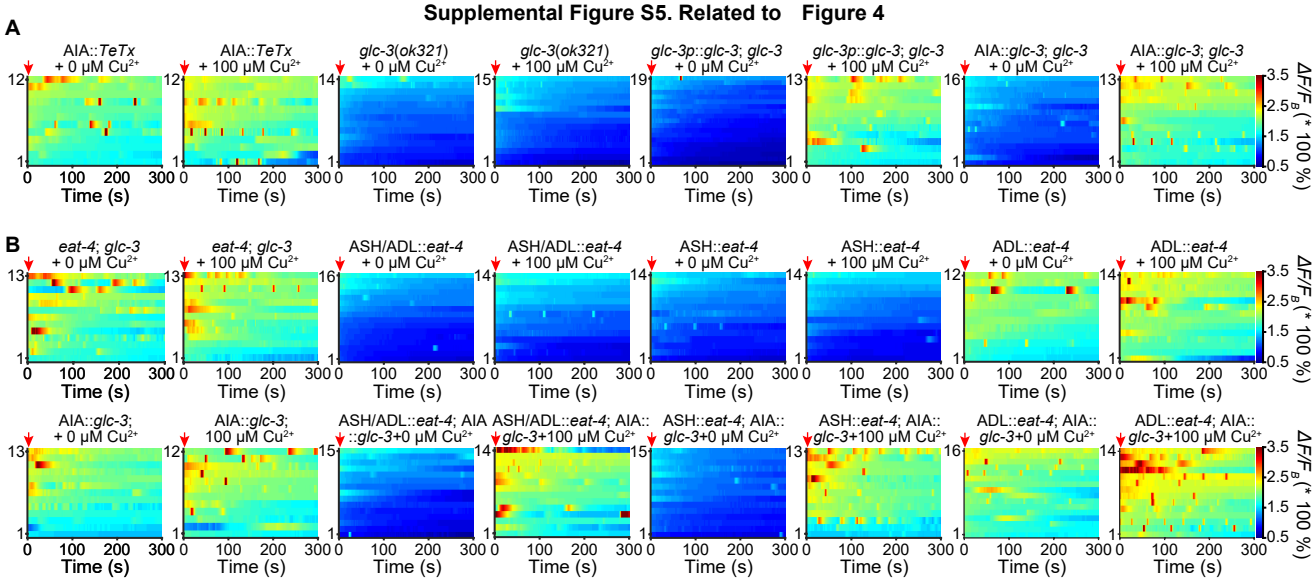

Figure S5. Changes in somal calcium transients in HSN motor neurons in the indicated worms treated without or with 100 μM $CuSO_4$. Related to figure 4.

(A and B) Heat maps of the percent changes in somal calcium transients in HSN motor neurons in the worms of indicated genotypes treated without or with 100 μM $CuSO_4$. Red arrows indicated the beginning time of the application of copper ion at concentrations indicated. $\Delta F = F - F_B$. F, the averaged fluorescence intensity of the region of interest (ROI) of an HSN soma in each frame; F_B, a background signal defined as the average fluorescence intensity of an ROI adjacent to the HSN soma in all frames. The label on the left y-axis indicates the number of tested worms.

The genotypes of tested worms are as follows: AIA::*TeTx*, *glc-3*(*ok321*), *glc-3p*::*glc-3*; *glc-3*(*ok321*), AIA::*glc-3*; *glc-3*(*ok321*), *eat-4*(*ky5*); *glc-3*(*ok321*), ASH/ADL::*eat-4*; *eat-4*(*ky5*); *glc-3*(*ok321*), ASH::*eat-4*; *eat-4*(*ky5*); *glc-3*(*ok321*), ADL::*eat-4*; *eat-4*(*ky5*); *glc-3*(*ok321*), AIA::*glc-3*; *eat-4*(*ky5*); *glc-3*(*ok321*), ASH/ADL::*eat-4*; AIA::*glc-3*; *eat-4*(*ky5*); *glc-3*(*ok321*), ASH::*eat-4*; AIA::*glc-3*; *eat-4*(*ky5*); *glc-3*(*ok321*) and ADL::*eat-4*; AIA::*glc-3*; *eat-4*(*ky5*); *glc-3*(*ok321*), respectively.

Supplemental Figure 6

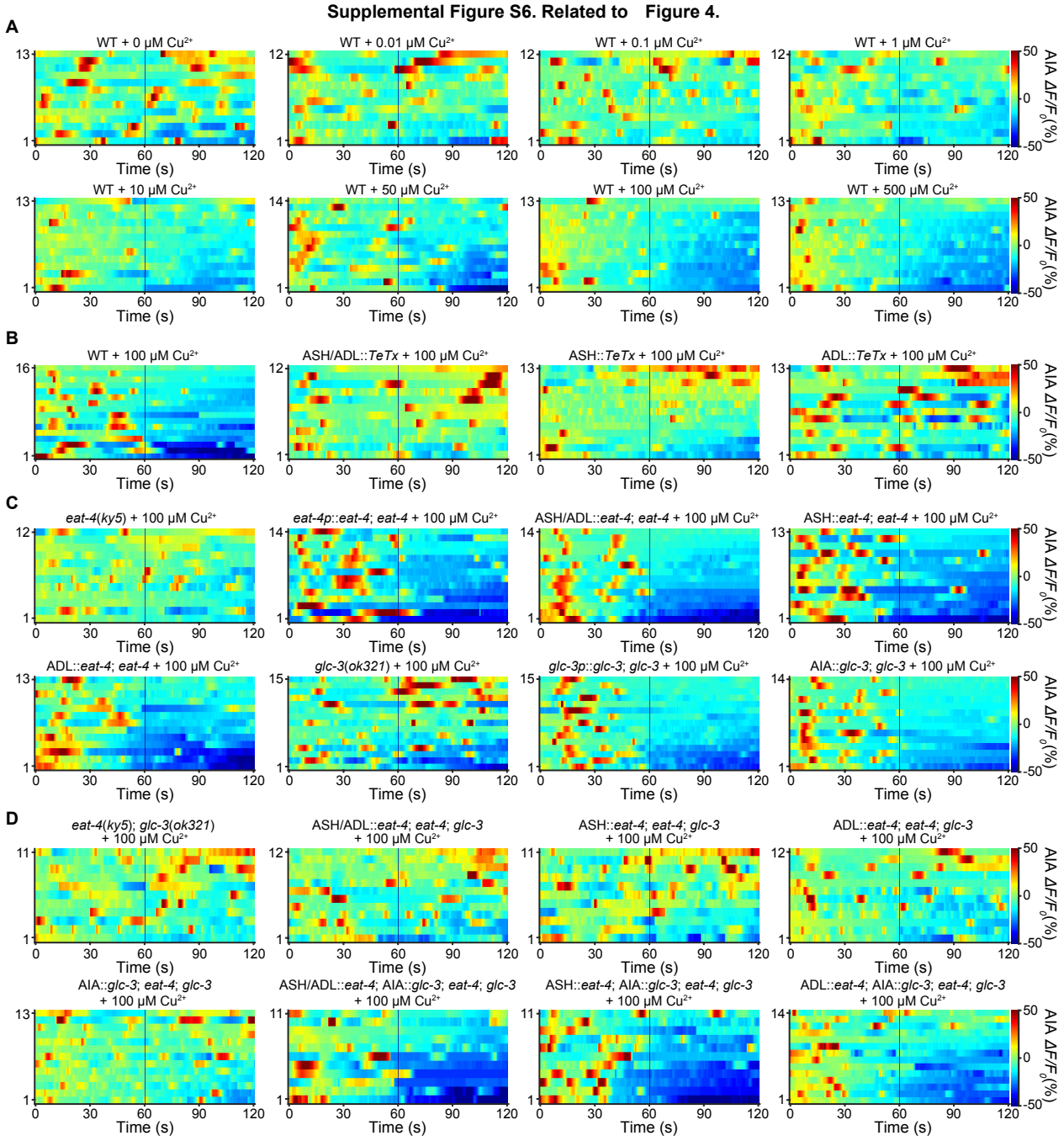

Figure S6. Changes in axonal calcium transients in AIA interneurons in the indicated worms treated with $CuSO_4$. Related to figure 4.

(A) Heat maps of percent changes in axonal Ca^{2+} transients evoked by stimulation of $CuSO_4$ at various concentrations in AIA interneurons in wild type (WT) N2 worms. The blue lines in the middle indicate the beginning time of the application of the $CuSO_4$ solution at concentrations indicated. $\Delta F = F - F_0$. F, the

averaged intensity of the region of interest (ROI) of an AIA axon in each frame that subtracted background fluorescence during chemical administration; F_0, that of the AIA axon within 60 s before stimulation. The label on the left y-axis indicates the number of tested worms.

(B–D) Heat maps of percent changes in axonal Ca^{2+} transients evoked by stimulation of 100 μM $CuSO_4$ in AIA interneurons in the worms of indicated genotypes. The blue lines in the middle indicate the beginning time of the application of the $CuSO_4$ solution at concentrations indicated.

The genotypes of tested worms are as follows: WT, ASH/ADL::*TeTx*, ASH::*TeTx*, ADL::*TeTx*, *eat-4*(*ky5*), *eat-4p*::*eat-4*; *eat-4*(*ky5*), ASH/ADL::*eat-4*; *eat-4*(*ky5*), ASH::*eat-4*; *eat-4*(*ky5*), ADL::*eat-4*; *eat-4*(*ky5*), *glc-3*(*ok321*), *glc-3p*::*glc-3*; *glc-3*(*ok321*), AIA::*glc-3*; *glc-3*(*ok321*), *eat-4*(*ky5*); *glc-3*(*ok321*), ASH/ADL::*eat-4; eat-4*(*ky5*); *glc-3*(*ok321*), ASH::*eat-4; eat-4*(*ky5*); *glc-3*(*ok321*), ADL::*eat-4; eat-4*(*ky5*); *glc-3*(*ok321*), AIA::*glc-3*; *eat-4*(*ky5*); *glc-3*(*ok321*), ASH/ADL::*eat-4*; AIA::*glc-3*; *eat-4*(*ky5*); *glc-3*(*ok321*), ASH::*eat-4*; AIA::*glc-3; eat-4*(*ky5*); *glc-3*(*ok321*) and ADL::*eat-4*; AIA::*glc-3; eat-4*(*ky5*); *glc-3*(*ok321*), respectively.

Supplemental Figure 7

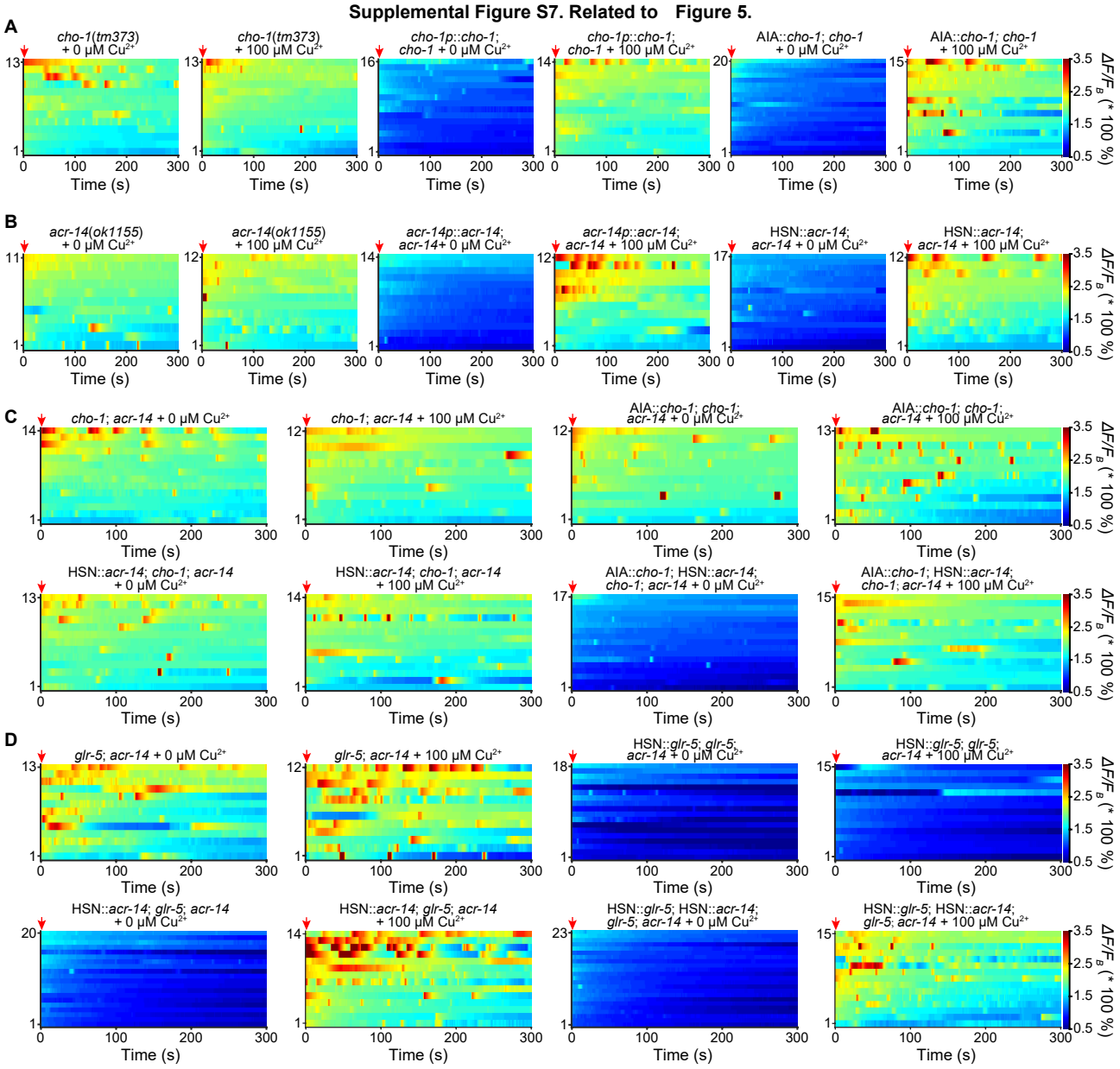

Figure S7. Changes in somal calcium transients in HSN motor neurons in the indicated worms treated without or with 100 μM $CuSO_4$. Related to Figure 5.

(A–D) Heat maps of percent changes in somal Ca^{2+} transients in HSN motor neurons in the worms of indicated genotypes treated without or with 100 μM $CuSO_4$. Red arrows indicated the beginning time of the application of $CuSO_4$ at concentrations indicated. $\Delta F = F - F_B$. F, the fluorescence intensity of the region of interest (ROI) of an HSN soma in each frame; F_B, a background signal defined as the average fluorescence intensity of a ROI adjacent to the HSN soma in all frames. Label on the left y-axis indicates the number of tested worms. The genotypes of tested worms are as follows: *cho-1*(*tm373*), *cho-1p*::*cho-1*; *cho-1*(*tm373*),

AIA::*cho-1*; *cho-1*(*tm373*), *acr-14*(*ok1155*), *acr-14p*::a*cr-14*; *acr-14*(*ok1155*), HSN::a*cr-14*; *acr-14*(*ok1155*), *cho-1*(*tm373*); *acr-14*(*ok1155*), AIA::*cho-1*; *cho-1*(*tm373*); *acr-14*(*ok1155*), HSN::a*cr-14*; *cho-1*(*tm373*); *acr-14*(*ok1155*), AIA::*cho-1*; HSN::a*cr-14*; *cho-1*(*tm373*); *acr-14*(*ok1155*), *glr-5*(*tm3506*); *acr-14*(*ok1155*), HSN::*glr-5*; *glr-5*(*tm3506*); *acr-14*(*ok1155*), HSN::a*cr-14*; *glr-5*(*tm3506*); *acr-14*(*ok1155*) and HSN::*glr-5*; HSN::a*cr-14*; *glr-5*(*tm3506*); *acr-14*(*ok1155*), respectively.

Supplemental Figure 8

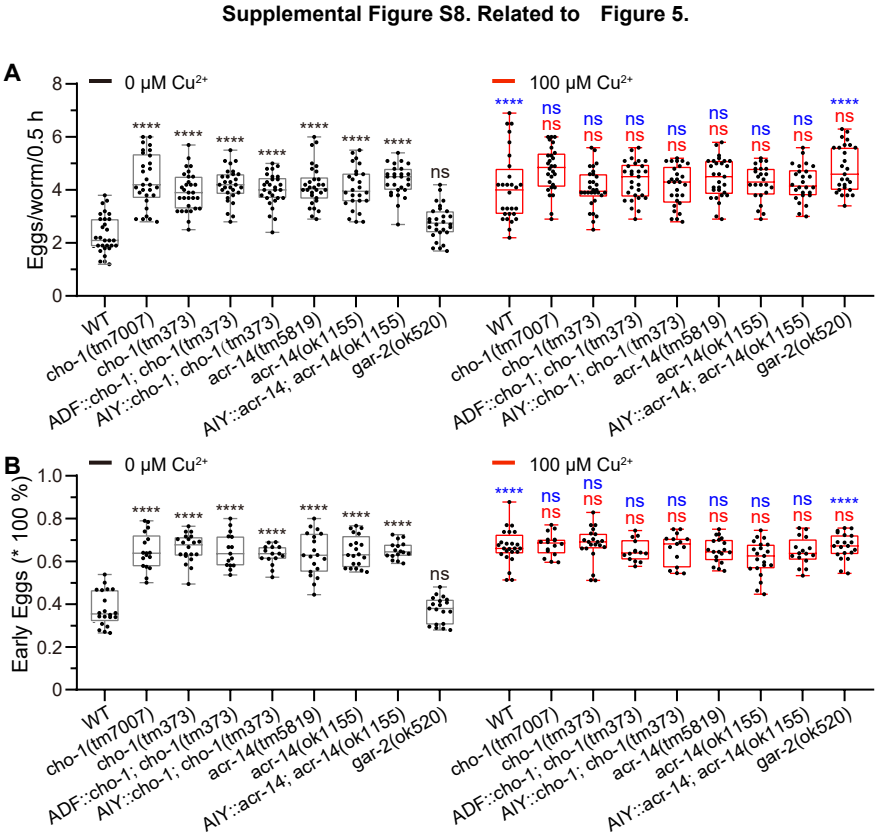

Figure S8. Screening of acetylcholine receptors and neurons to test whether they involve in the regulation of egg-laying. Related to figure 5.

(A–B) The number of the eggs laid per worm per 30 min (egg-laying rate, A) and percent of the eggs at early developmental stages (stages of 1–8 cells and 9–20 cells, B) in worms of the indicated genotypes treated without (in black) or with (in red) 100 μM $CuSO_4$. The genotypes of tested worms are as follows: wild type N2 (WT as a control), *cho-1*(*tm7007*), *cho-1*(*tm373*), ADF::*cho-1*; *cho-1*(*tm373*), AIY::*cho-1*; *cho-1*(*tm373*), *acr-14*(*tm5819*), *acr-14*(*ok1155*), AIY::*acr-14*; *acr-14*(*ok1155*) and *gar-2*(*ok520*), respectively.

All data were displayed as box plots with each dot representing the data from each individual tested worm. Statistical significance of difference was analyzed by two-way ANOVA analysis with the post hoc test of Tukey's multiple comparison correction and indicated as follows: ns = not significant, **** $P < 0.0001$, and in different colors for varied comparisons. Black or red, a comparison of tested worms with control under Cu^{2+}-untreated or Cu^{2+}-treated condition; blue, that of Cu^{2+}-untreated with Cu^{2+}-treated worms of the same genotype.

Supplemental Figure 9

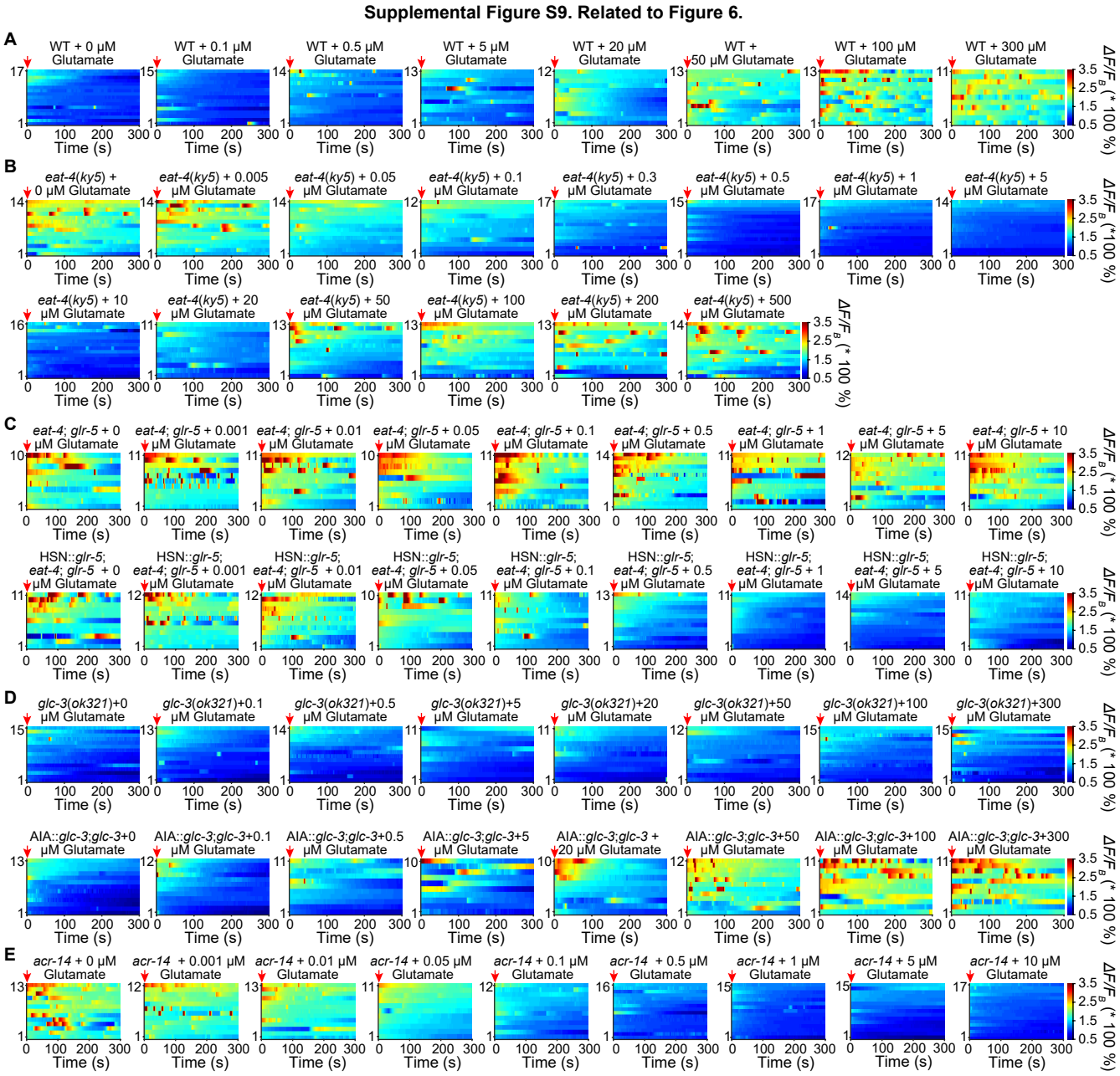

Figure S9. Changes in somal calcium transients in HSN motor neurons in the indicated worms treated without or with exogenous glutamate at various concentrations. Related to figure 6.

（A-E）Heat maps of percent changes in somal Ca^{2+} transients in HSN motor neurons in wild type N2 (WT), mutant, and transgenes of indicated genotypes treated without or with exogenous glutamate at various concentrations showed, respectively. Red arrows indicated the beginning time of the application of glutamate at concentrations indicated. $\Delta F = F - F_B$. F, the averaged fluorescence intensity of the region of interest (ROI) of an HSN soma in each frame; F_B, a background signal defined as the average fluorescence

intensity of an ROI adjacent to the HSN soma in all frames. The label on the left y-axis indicates the number of tested worms.

The genotypes of tested worms are as follows: *eat-4*(*ky5*), *eat-4*(*ky5*); *glr-5*(*tm3506*), HSN::*glr-5*; *eat-4*(*ky5*); *glr-5*(*tm3506*), *glc-3*(*ok321*), AIA::*glc-3*; *glc-3*(*ok321*) and *acr-14*(*ok1155*), respectively.

Supplemental Figure 10

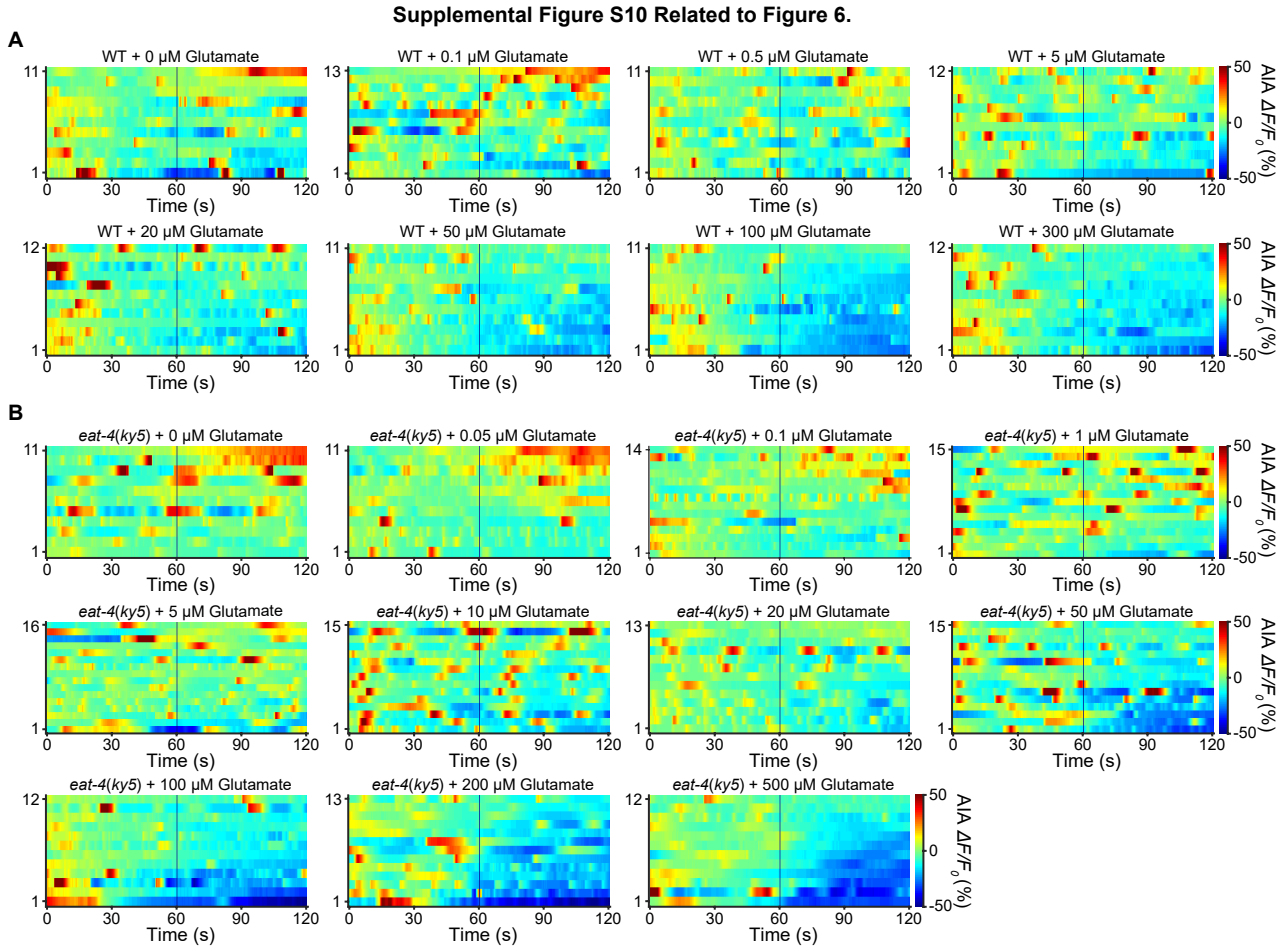

Figure S10. Changes in axonal calcium transients in AIA interneurons in worms treated without or with exogenous glutamate at various concentrations. Related to figure 6.

(A and B) Heat maps of percent changes in axonal Ca^{2+} transients in AIA interneuron in wild type N2 (WT, as a control) and mutant worms of indicated genotypes treated without or with exogenous glutamate at various concentrations as shown, respectively. The blue lines in the middle indicate the beginning time of the application of glutamate solution at concentrations indicated.

$\Delta F = F - F_0$. F, the averaged fluorescence intensity (average background signal subtracted) of the region of interest (ROI) of an AIA axon in each frame during chemical administration; F_0, that within 60 s before stimulation. The label on the left y-axis indicates the number of tested worms.

Supplemental Figure 11

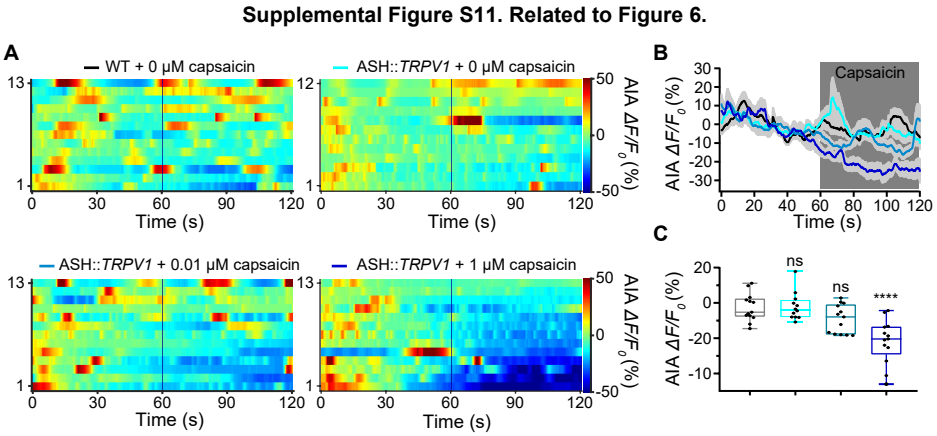

Figure S11. Chemogenetically activating sensory ASH neurons suppressed Ca^{2+} signals in AIA interneurons. Related to figure 6.

(A) Heat maps of percent changes in axonal Ca^{2+} transients in AIA interneuron in ASH::*TRPV1* transgenic worms treated without or with exogenous capsaicin at different concentrations. $\Delta F = F - F_0$. F, the averaged fluorescence intensity (average background signal subtracted) of the region of interest (ROI) of an AIA axon in each frame during chemical administration; F_0, that within 60 s before stimulation. The label on the left y-axis indicates the number of tested worms. The blue lines in the middle indicate the beginning time of the application of capsaicin solution at concentrations indicated.

(B) Curves of axonal Ca^{2+} signals in AIA interneurons in ASH::*TRPV1* transgenic worms treated without or with exogenous capsaicin at different concentrations indicated. Data were expressed as the means ± SEM, as indicated by solid traces ± grey shading.

(C) Axonal Ca^{2+} signals in AIA interneurons in ASH::*TRPV1* transgenic worm treated without or with exogenous capsaicin at different concentrations. Data were expressed as box-plots with each dot representing the data from each individual tested animal. The significance of statistic difference was analyzed by one-way ANOVA with the post hoc test of Dunnett's multiple comparisons correction and indicated as ns = not significant, **** $P < 0.0001$, in comparison with those in wild type N2 worm without capsaicin treatment.

TRANSPARENT METHODS

***C. elegans* Strains.** *C. elegans* strains were cultured on nematode growth media (NGM) plates at 20°C, using *E. coli* bacteria OP50 as food according to standard methods (Brenner, 1974). The strains were obtained from the Caenorhabditis Genetics Centre (CGC, http://www.cbs.umn.edu/CGC/) or the National BioResources Project (NBRP, http://www.shigen.nig.ac.jp/c.elegans/index.jsp). Double mutant animals were made using standard genetic techniques (Brenner, 1974) and identified by PCR or sequencing. All transgenic strains were generated using published methods (Mello et al., 1991). Plasmids were injected at 50 ng/μl together with *lin-44p*::*GFP* (10 ng/μl) or *vha-6p*::*GFP* (10 ng/μl) as a co-injected gene marker. All strains used in this study are listed in Excel-format Table S1. We used two or three lines of transgenic worms to conduct the experiments and summarized all data for statistical analysis.

Molecular Cloning. All expression constructs were generated with the Three-Fragment Multisite Gateway system (Invitrogen, Camarillo, CA, USA). Briefly, three entry clones comprising three PCR products ("A" for a promoter, "B" for the gene of interest and "C" for *sl2*::*TagRFP-t* or *sl2*::*GFP* or *3′* UTR, respectively) were recombined into the pDEST™ R4-R3 Vector II or custom-modified destination vectors using *att*L4-*att*R recombination reactions to generate expression clones.

We constructed an "A" entry clone containing a sequence of the promoter used in this study by the In-Fusion method. In short, a modified *att*L4-*att*R1 entry clone was linearized by PCR reaction. Then, used linearized product and PCR product of a promoter to generate "A" entry clones, using ClonExpress®Ⅱ One Step Cloning Kit (Vazyme Biotech Co., Ltd, Nanjing, China). PCR product of a promoter was amplified from *C. elegans* genome DNA, with primers containing 15–20 bp sequences that carry a part of *att*L4 and *att*R1 recombination sites. Alternatively, vectors of *C. elegans* Promoters Library (Thermo Fisher Scientific, Waltham, MA, USA) were directly used. The length of each promoter used in this study is as follows: *osm-9p* 3 kb, *ocr-2p* 2.51 kb, *sra-6p* 3.8 kb, *ver-2p* 2.72 kb, *gpa-4p* 2.5 kb, *gpa-11p* 3.3 kb, *srh-142p* 3.5 kb, *egl-6*(*a*)*p* 3.4 kb, *gcy-28*(*d*)*p* 2.8 kb, *npr-9p* 1.7 kb, *T19C4.5p* 4 kb, *sra-9p* 3 kb, *gcy-15p* 0.69 kb, *odr-7p* 5 kb, *str-1p* 4 kb, *str-199p* 0.44 kb, *srh-11p* 0.65 kb, *eat-4p* 2 kb, *glc-3p* 2 kb, *cho-1p* 2 kb, *acr-14p* 2 kb and *glr-5p* 5 kb. All primers for cloning these promoters are listed in Table S2.

The extrachromosomal expression of the tested genes was driven by promoters as follows: *ver-2p* in ADLs, *gpa-4p* in ASIs, *gpa-11p* in ASHs/ADLs, *srh-142p* in ADFs, *egl-6*(*a*)*p* in HSNs (Emtage et al., 2012; Ringstad and Horvitz, 2008), *gcy-28*(*d*)*p* in AIAs, *npr-9p* in AIBs, *T19C4.5p* in AIYs, *sra-9p* in ASKs, *gcy-15p* in ASGs, *odr-7p* in AWAs, *str-1p* in AWBs, *str-199p* in AWCs and *srh-11p* in ASJs. For neuron-specific expression of *osm-9*, *ocr-2*, *TeTx*, *TRPV1* and *eat-4* in ASH neurons, we employed a FLP–FRT site-specific recombination (FLP-out) system as previously reported (Davis et al., 2008; Guo et al., 2015; Macosko et al., 2009; Voutev and Hubbard, 2008). We used fusion PCR to get a fragment of *attB1*::*FRT*::*stop*::*FRT*::*gene*::*attB2*, then use BP reactions to construct slot2 donor vectors. Using LR reactions, we generated the following listed expression plasmids: *gpa-11p*::*FRT*::*stop*::*FRT*::*osm-9*::*sl2*::*GFP*, *gpa-11p*::*FRT*::*stop*::*FRT*::*ocr-2*::*sl2*::*GFP*, *gpa-11p::FRT*::*stop*::*FRT*::*TeTx*::*sl2*::*GFP*, *gpa-11p::FRT*::*stop*::*FRT*::*TRPV1*::*sl2*::*GFP* and *gpa-11p::FRT*::*stop*::*FRT*::*eat-4*::*sl2*::*GFP*. The expression patterns of *gpa-11* and *sra-6* were ASHs/ADLs and ASHs/ASIs, respectively. Ultimately, the genes of *osm-9*, *ocr-2*, TeTx, TRPV1 and *eat-4* were specifically expressed in ASH neurons through the co-injection of the plasmids *sra-6p*::*flp* and *gpa-11p*::*FRT*::*stop*::*FRT*::*osm-9*::*sl2*::*GFP*, *sra-6p*::*flp* and *gpa-11p::FRT*::*stop*::*FRT*::*ocr-2*::*sl2*::*GFP*, *sra-6p*::*flp* and *gpa-11p*::*FRT*::*stop*::*FRT*::*TeTx*::*sl2*::*GFP*, *sra-6p*::*flp* and *gpa-11p*::*FRT*::*stop*::*FRT*::*TRPV1*::*sl2*::*GFP* and *sra-6p*::*flp* and *gpa-11p*::*FRT*::*stop*::*FRT*::*eat-4*::*sl2*::*GFP*, respectively. Each core construct and two plasmids for recombinases were co-injected at 30 ng/μl for each construct.

BP recombination reactions were used to generate the entry clones B (containing a sequence of a tested gene) and C (containing *unc-54 3′* UTR or *sl2-GFP*). The following genes were used to create the B entry clones. The genes *osm-9* (2814 bp), *ocr-2* (2703 bp), *glc-3* (1455 bp), *cho-1* (1731 bp), *acr-14* (1503 bp), *glr-5* (2799 bp), and *eat-4* (1731 bp) were amplified from mixed-stage N2 worm genomic cDNA by PCR, with primers listed in Table S2. Their PCR products flanked by *att*B1 and *att*B2 were recombined with the pDONR-221 vector containing *att*P1 and *att*P2. To generate the entry clone C, the BP reaction sites *att*B2r and *att*B3 were inserted in the sequences of *sl2-GFP* or *unc-54 3′* UTR, and were recombined with PDONR-P2R-P3 vector.

Egg-laying assays. We used day-1 adult worms and performed all behavioral tests on agar plates seeded with *E. coli* OP50 bacteria at room temperature between approximately 20 and 22°C. We synchronized the tested worms by picking 30–40 egg-laying adults into a culture dish coated with *E. coli* OP50 bacteria cultured in 2 × yeast tryptone (YT) medium and let the

worms lay eggs for 3–4 h. The YT medium consists of (per liter) 16 g tryptone, 10 g yeast extract, 5 g NaCl (pH 7.2, adjusted by 1 M HCl or 1M NaOH). Then picked up the adult animals and made the laid eggs hatch and larvae grow to day-1 adults. We transferred ten day-1 adult worms onto each test NGM plate (3.5 cm in diameter) seeded with OP50 bacteria, and let animals move and lay eggs freely for a given time (30 min for most tests, or various time in minutes of 5, 10, 20, 30, 45, 60, 120, 180, 240, 300 and 360 for the time course test of Cu^{2+}-treatment on egg-laying). For eliminating the interference of the worm picking process on tests, we removed the eggs laid in the first 3 minutes. After the given time, we removed the worms from the assay plate and counted the number of eggs under a stereomicroscope.

We examined the embryonic stage of eggs under a stereomicroscope and categorized as 1–8 cells, 9–20 cells, 21+ cells, comma, two-folds, and three-folds+, as previously described (Ringstad and Horvitz, 2008). Our tests (Figure 1C) showed that Cu^{2+}-treated animals displayed a significant difference in ratios of early embryonic stages of 1–8 and 9–20 cells. So we summated the data in the two phases and expressed them as early eggs (Figure 1D), excepted in Figure 1C.

For the pharmacological tests, the test plates were added with $CuSO_4$, $NiCl_2$, $MnCl_2$, $Fe_2(SO_4)_3$, glutamate, or capsaicin and seeded with OP50 bacteria. To prepare dishes containing chemicals at the final concentrations used for the tests, we added the solutions of chemicals dissolved in M13 buffer into the agar solution at approximately 60°C before making the plates and used the same amount of vehicle to prepare dishes for the control tests. M13 buffer solution consists of (in mM) Tris 30, NaCl 100, and KCl 10 (pH 7.2, adjusted by 1M HCl or 1M NaOH).

Specific manipulation of tested neurons. We employed neuron-specific extrachromosomal expression of TeTx to genetically block vesicle fusion with the plasma membrane and thus neurotransmitter release in the tested neurons. TeTx is a specific protease of synaptobrevin (Schiavo et al., 1992). It is used successfully to inhibit chemical synaptic transmission of tested neurons in *C. elegans* (Guo et al., 2015; Liu et al., 2019; Macosko et al., 2009; Wang et al., 2016). For chemogenetic activation of tested neurons, we used FLP-out system or neuron-specific promoters to drive specific expression of rat *TRPV1* gene in the tested neurons and employed capsaicin to activate the channel.

For the preparation of the test NGM plates containing capsaicin, we diluted the stock solution of capsaicin (25 mM in ethanol) with ultrapure water into a 1 mM working solution. We then added a certain amount of working solution needed for the final concentration used in this study into the agar solution at approximately 60°C before making the plates. For the

control test, we put the same amount of ethanol as that in the capsaicin test solution into the agar solution to make the dishes.

Calcium imaging. We measured the calcium transients of tested neurons by detecting changes in the fluorescence intensity of calcium indicator GCaMP3.0. We excited GCaMP3.0 with 460-470 nm light emitted by an Osram Diamond Dragon LBW5AP light-emitting diode (LED) model (Osram, Marcel-Breuer-Straße 6, Munich, Germany) constructed in a multi-LED light source (MLS102, InBio Life Science Instrument Co. Ltd., Wuhan, China), and filtered its fluorescence with a Semrock FF01-520/35-25 emission filter (IDEX Health & Science, LLC, Oak Harbor, WA, USA) under an Olympus IX-70 inverted microscope (Olympus, Tokyo, Japan) equipped with a 40× objective lens (numerical aperture (NA) = 1.3, Carl Zeiss MicroImaging GmhH, Göttingen, Germany). We employed Day-1 adult worms for all calcium imaging and used an animal only once. Because *C. elegans* worms are sensitive to the blue light used for Ca^{2+} imaging, we exposed the tested animal with fluorescent excitation light for 1 min before recording to decrease the light impact on Ca^{2+} fluorescence for all Ca^{2+} fluorescence imaging tests.

For Ca^{2+} fluorescence imaging in HSNs, we used an immobilized animal as described previously (Zhang et al., 2008). We glued the tested worm onto a thin PDMS pad attached to a cover-glass with histoacryl. We immersed the worm's body in OP50 solution at OD_{600} = 0.9 made in M13 buffer before fluorescence recording. After 1 min of exposure to the excitation light, we started to record the Ca^{2+} fluorescence of HSN in worms immersed in M13 buffer with food or a test solution for 5 min. For tests of control or those under standard conditions, we used M13 buffer with food to immerse the tested worm. In contrast, for chemical treatment tests, we employed a test solution of $CuSO_4$ or glutamate at varied concentrations made in M13 buffer with food to immerse the tested animal.

For calcium imaging tests in AIA interneurons and ADL neurons, we used fluorescence microscopy combined with a microfluidic device to fix the test worm, as described previously (Chronis et al., 2007; Guo et al., 2015; Liu et al., 2019; Wang et al., 2016; Wang et al., 2015). Briefly, we transferred a worm from the agar plate with food into the M13 buffer solution to wash bacteria off its body. Then, loaded worm into a homemade PDMS microfluidic chip with its nose exposed to buffer under laminar flow. We automatically switch the perfusion of solutions used via programmable automatic drug-feeding equipment (MPS-2, InBio Life Science Instrument Co. Ltd.), and employed M13 buffer and solutions of $CuSO_4$ and glutamate (Sigma) at various concentrations made in M13 buffer for control test or chemical

treatment tests, respectively. We fluorescently imaged the Ca^{2+} fluorescence with an Andor iXon^{EM}+ DU885K EMCCD camera at a resolution of 256 × 256 pixels and a rate of 10 frames per second.

We used Image-Pro Plus 6.0 (Media Cybernetics, Inc., Rockville, MD, USA) to capture the fluorescence intensity of the region of interest (ROI) of soma of HSN motor neurons and ADL sensory neurons or an axon of AIA interneurons in each frame. Then averaged the signals, and used the average background signal F_B of an adjacent ROI in all frames to subtract the background fluorescence. We used ΔF $(F - F_B)/F_B$ or ΔF $(F - F_0)/F_0$ to calculate the Ca^{2+} signals in the soma of HSNs or those in the axon of AIAs and the soma of ADLs. F, the average background signal (F_B)-subtracted fluorescence intensity during chemical administration; F_0, that within the last 30 s and 10 s before stimulation for AIAs and ADLs, respectively. We displayed percent changes in fluorescence intensity with heat maps, curves (the means ± SEM at solid color trace and grey shadow), or box plots.

Confocal fluorescence imaging. Confocal fluorescence imaging was performed by use of an Andor (Andor Technology plc., Springvale Business Park, Belfast, UK) Revolution XD laser confocal microscope system based on a spinning-disk confocal scanning head CSU-X1 (Yokogawa Electric Corporation, Musashino-shi, Tokyo, Japan), under the control of the Andor IQ 1.91 software. The confocal system was mounted on an Olympus IX-71 inverted microscope (Olympus, Tokyo, Japan). Live young adult worms were mounted on a 2% (w/v) agarose pad with 10 mM levamisole (Sigma-Aldrich). The fluorescent images were imaged by a 60 × objective lens (numerical aperture NA = 1.45, Olympus) and captured by an Andor iXon^{EM}+ DU-897D EMCCD camera. The images were displayed using Image J 1.52o software (Wayne Rasband, National Institutes of Health, USA).

Quantification and statistical analysis. The number of the eggs laid in a given period (egg-laying rate) and percent of the egg at early developmental stages (stages of both 1–8 cells and 9–20 cells) were displayed as box plots with each dot representing the data from each individual tested worm or as the means ± SEM. The data for Ca^{2+} signals were expressed as heat maps, box plots, or as the means ± SEM indicated by solid traces ± grey shading. Data were statistically analyzed by the use of software packages in GraphPad Prism 8 (GraphPad Software, Inc., San Diego, CA, USA) and described in figure legends. When the comparison was limited to between 2 groups, an unpaired *t*-test was used to analyze differences and to calculate *P*-values. When more than two groups of data were compared, data were analyzed

by ordinary one-way or two-way ANOVA (analysis of variance), with recommended post hoc tests in the GraphPad Prism 8 software package. Dunnett's multiple comparison correction was applied when multiple samples were compared to a single sample, i.e., wild type N2 or other control, and Tukey's multiple comparison correction was used when multiple samples were compared among themselves. The *P*-value was indicated as follows: ns = not significant, * $P < 0.05$, ** $P < 0.01$, *** $P < 0.001$, **** $P < 0.0001$, and in different colors for varied comparisons. Black, a comparison of tested worm with control under standard culture conditions; red, that of tested worm with control under Cu^{2+} challenges; blue, that of Cu^{2+}-untreated worm with Cu^{2+}-treated animal of the same genotype.

Supplemental Tables

Table S2. List of oligonucleotides used in this study, Related to METHODS.

Genes	Forward primers	Reverse primers
acr-14(cDNA)	TGTACAAAAAAGCAGGCTTAATGTCTTTGTTTTCTTTA	GTACAAGAAAGCTGGGTATCTTAAATGTTTGCCAGTATATG
acr-14p	GTTGCTCCAAGCTTTTCCCCAGAAAAATCGCCAG	CTTGCACGACTAGTCATCAAGTATTAACCGAAAAC
cho-1(cDNA)	GTACAAAAAAGCAGGCTTAATGGCCGACTTATTGGG	GTACAAGAAAGCTGGGTATCTTAATTGCTATTTGTGG
cho-1p	GTTGCTCCAAGCTTGGTTTCAAAAATGAAATCATTC	CTTGCACGACTAGTTATTTGTCCTGGAAAATTAAAATTG
eat-4(cDNA)	GTACAAAAAAGCAGGCTTAATGTCGTCATGGAACGAGG	GTACAAGAAAGCTGGGTATCCTACCACTGCTGATAATG
eat-4p	GTTGCTCCAAGCTTATTTCTAATAAAACGGTCTAC	CTTGCACGACTAGTCATGGTTTCTGAAAATGATG
eft-3p	GTTGCTCCAAGCTTGCACCTTTGGTCTTTTATTG	CTTGCACGACTAGTTGAGCAAAGTGTTTCCCAAC
egl-6(*a*)*p*	GTTGCTCCAAGCTTTAAAAAATTCGATCAAG	CTTGCACGACTAGTTTTTTCACTCTTTCACG
gcy-15p	GTTGCTCCAAGCTTGTTATCCTAATAGCAAC	CTTGCACGACTAGTAGCTGATGGGATGTAGGC
gcy-28(*d*)*p*	GTTGCTCCAAGCTTTACAATTGTAGTGAGCTTC	CTTGCACGACTAGTTTCGCACTCATCTCACC
glc-3(cDNA)	GTACAAAAAAGCAGGCTTAATGAGTCTCCGTTCACTTC	GTACAAGAAAGCTGGGTATCTCATTTGGCTTCCGGTGC
glc-3p	GTTGCTCCAAGCTTTTCCCCAGAAAAATCGCCAG	CTTGCACGACTAGTCATCAAGTATTAACCGAAAAC
glr-5(cDNA)	GTACAAAAAAGCAGGCTTAATGCAGTTTAATAACAAC	GTACAAGAAAGCTGGGTATCTCAAATTGTTGTTTTTTTAAG
glr-5p	GTTGCTCCAAGCTTGTATTTCTTACTTGTATTTTC	CTTGCACGACTAGTGATGCTTATTATTCACATG
gpa-11p	GTTGCTCCAAGCTTATTGCCGCCCGCAAAATATCGTATT	CTTGCACGACTAGTCATTTTTGGCTGAAAATGGAGAAGT
gpa-4p	GTTGCTCCAAGCTTTGCGACTTTCGATACGTAGGTC	CTTGCACGACTAGTTGTTGAAAAGTGTTCACAAAATGA
npr-9p	GTTGCTCCAAGCTTGTTGGGTTGATGACGACG	CTTGCACGACTAGTGCTCTAAAATTACAATAAAG
ocr-2(cDNA)	GTACAAAAAAGCAGGCTTATTCCTCATCTTCA	GTACAAGAAAGCTGGGTATCAGTGAGCAGCACCATTTCCA
ocr-2p	GTTGCTCCAAGCTTAGAAGAGTCAACATTGTAC	CTTGCACGACTAGTCTTAATGATGTGATGTACTC
odr-7p	GTTGCTCCAAGCTTCAGAGTTCCTCACATTTAT	CTTGCACGACTAGTTTTTTGAAAGGAAATAGCTG
osm-9(cDNA)	GTACAAAAAAGCAGGCTTACGGTGGAAGTTCG	GTACAAGAAAGCTGGGTATCATTCGCTTTTGTCATTTGT
osm-9p	GTTGCTCCAAGCTTCCAAACATGGGCGGTGGAA	CTTGCACGACTAGTATTGCTATATTCTAGGTATTGC
sra-6p	GTTGCTCCAAGCTTACTGACTGGGCCGGCCCC	CTTGCACGACTAGTGGAGCAGCACAACTTAAA
sra-9p	GTTGCTCCAAGCTTGCATGCTATATTCCACCAA	CTTGCACGACTAGTTTCTATGATTGATGCACAAG
srh-11p	GTTGCTCCAAGCTTGGGCAAGGACAATGTTGCCG	CTTGCACGACTAGTTGGGAATAAAATAACGACG
srh-142p	GTTGCTCCAAGCTTTTCATTTCTCAATTTTCTAGCAAAC	CTTGCACGACTAGTATTGGCAAAAAGAAAAAAGAGGTGC
str-199p	GTTGCTCCAAGCTTCTCCGTTGATTGTCCAAATGT	CTTGCACGACTAGTGTCATGAAAAATTTCCAAG
str-1p	GTTGCTCCAAGCTTGAGTGAGAAGAATGTCACGACT	CTTGCACGACTAGTCATTAGTCAAATGATATGAAGTTTG
T19C4.5p	GTTGCTCCAAGCTTGAATGCAATATTGAAACACTTGCAA	CTTGCACGACTAGTCATTTCTTACCGTAACCCACA
ver-2p	GTTGCTCCAAGCTTTAAATAAAACGTAATATATTG	CTTGCACGACTAGTCATGCAATTTAGTTTTTTATAC

References

Brenner, S. (1974). The genetics of *Caenorhabditis elegans*. Genetics *77*, 71-94.

Chronis, N., Zimmer, M., and Bargmann, C.I. (2007). Microfluidics for in vivo imaging of neuronal and behavioral activity in *Caenorhabditis elegans*. Nat Methods *4*, 727-731.

Davis, M.W., Morton, J.J., Carroll, D., and Jorgensen, E.M. (2008). Gene activation using FLP recombinase in *C. elegans*. PLoS Genet *4*, e1000028.

Emtage, L., Aziz-Zaman, S., Padovan-Merhar, O., Horvitz, H.R., Fang-Yen, C., and Ringstad, N. (2012). IRK-1 potassium channels mediate peptidergic inhibition of *Caenorhabditis elegans* serotonin neurons via a G_o signaling pathway. J Neurosci *32*, 16285-16295.

Guo, M., Wu, T.H., Song, Y.X., Ge, M.H., Su, C.M., Niu, W.P., Li, L.L., Xu, Z.J., Ge, C.L., Al-Mhanawi, M.T.H.*, et al.* (2015). Reciprocal inhibition between sensory ASH and ASI neurons modulates nociception and avoidance in *Caenorhabditis elegans*. Nat Commun *6*, e5655.

Liu, H., Qin, L.W., Li, R., Zhang, C., Al-Sheikh, U., and Wu, Z.X. (2019). Reciprocal modulation of 5-HT and octopamine regulates pumping via feedforward and feedback circuits in *C. elegans*. Proc Natl Acad Sci U S A *116*, 7107-7112.

Macosko, E.Z., Pokala, N., Feinberg, E.H., Chalasani, S.H., Butcher, R.A., Clardy, J., and Bargmann, C.I. (2009). A hub-and-spoke circuit drives pheromone attraction and social behaviour in *C. elegans*. Nature *458*, 1171-1175.

Mello, C.C., Kramer, J.M., Stinchcomb, D., and Ambros, V. (1991). Efficient gene transfer in *C.elegans:* extrachromosomal maintenance and integration of transforming sequences. EMBO J *10*, 3959-3970.

Ringstad, N., and Horvitz, H.R. (2008). FMRFamide neuropeptides and acetylcholine synergistically inhibit egg-laying by *C. elegans*. Nat Neurosci *11*, 1168-1176.

Schiavo, G., Benfenati, F., Poulain, B., Rossetto, O., Polverino de Laureto, P., DasGupta, B.R., and Montecucco, C. (1992). Tetanus and botulinum-B neurotoxins block neurotransmitter release by proteolytic cleavage of synaptobrevin. Nature *359*, 832-835.

Voutev, R., and Hubbard, E.J. (2008). A "FLP-Out" system for controlled gene expression in *Caenorhabditis elegans*. Genetics *180*, 103-119.

Wang, W., Qin, L.W., Wu, T.H., Ge, C.L., Wu, Y.Q., Zhang, Q., Song, Y.X., Chen, Y.H., Ge, M.H., Wu, J.J.*, et al.* (2016). cGMP signalling mediates water sensation (hydrosensation) and hydrotaxis in *Caenorhabditis elegans*. Sci Rep *6*, 19779.

Wang, W., Xu, Z.J., Wu, Y.Q., Qin, L.W., Li, Z.Y., and Wu, Z.X. (2015). Off-response in ASH neurons evoked by $CuSO_4$ requires the TRP channel OSM-9 in *Caenorhabditis elegans*. Biochem Biophys Res Commun *461*, 463-468.

Zhang, M., Chung, S.H., Fang-Yen, C., Craig, C., Kerr, R.A., Suzuki, H., Samuel, A.D., Mazur, E., and Schafer, W.R. (2008). A self-regulating feed-forward circuit controlling *C. elegans* egg-laying behavior. Curr Biol *18*, 1445-1455.